

REVIEW ARTICLE

Open Access

NFC/RFID-enabled wearables and implants for biomedical applications

Haochen Zou¹, Zhibo Zhou¹, Mengyao Huang², Wenhao Li¹, Bowen Yang¹, Xiao Zhao¹, Ting Li¹, Lijie Xu²✉, Ting Wang¹✉ and Lianhui Wang¹✉

Abstract

Near Field Communication (NFC) and Radio Frequency Identification (RFID) technologies offer wireless data transmission and energy supply for flexible wearable and implantable sensing systems. By eliminating bulky batteries or external wiring, these technologies significantly advance personalized medicine through wearable and implantable systems with reduced size, increased flexibility, and improved mechanical adaptability to the human body. This multidisciplinary research area encompasses the fundamental mechanisms of antenna theory, simulation & design, micro/nano-fabrication, and their biomedical applications. This review provides an overview of emerging wireless, personalized/decentralized biomedical devices focusing on NFC/RFID antennas design mechanisms, flexible NFC/RFID-based physical, chemical, and biosensors, as well as drug delivery implants. Moreover, challenges and future directions regarding flexible NFC/RFID-based systems are provided. Advancing this field will require collaborative efforts from researchers in antenna design, materials science, biology, and medical care, driving the development of NFC/RFID in biomedical applications.

Introduction

Wearable and implantable biosensors have emerged as a prominent field of research in recent years, which provide access to physiological signals and are of great significance for the diagnosis and treatment of diseases¹. Ongoing advancements in medicine and healthcare have led to widespread applications of these devices, primarily in health monitoring^{2–7}, postoperative evaluation^{8–10}, drug delivery^{11,12} and more. For instance, smart wearable devices can effectively monitor various physiological parameters, such as heart rate¹³, blood pressure¹⁴ and body temperature¹⁵. Given that wearable devices need to be worn without disrupting the wearer's daily life, there is a requirement for miniaturization and flexibility. In

addition, implantable devices requiring surgical implantation must minimize discomfort and ensure robust biocompatibility to prevent adverse reactions such as inflammation or immune responses.

Traditional sensors often rely on wire-connections or batteries for power supply, which not only limits their miniaturization and flexibility, but also can pose a potential risk of infection, consequently restricting their applications in wearable and implantable scenarios¹⁶. To address these limitations, wireless data transmission technology such as Near Field Communication /Radio Frequency Identification (NFC/RFID) emerges as a promising solution. NFC is a short-range wireless technology designed for near-field interactions (typically less than 10 cm), supporting bidirectional data transmission and encryption protocols for high security^{17,18}. It is commonly adopted in high-security applications such as mobile payments and smart device pairing. In comparison, RFID operates across low-frequency (LF, 30 kHz-300 kHz), high-frequency (HF, 3 MHz-30 MHz), and ultra-high-frequency (UHF, 300 MHz-3 GHz) bands, with communication distances ranging from near-field (centimeter-level) to far-field (tens of meters). It primarily enables

Correspondence: Lijie Xu (xulj@njupt.edu.cn) or Ting Wang (iamtingwang@njupt.edu.cn) or Lianhui Wang (iamlhwang@njupt.edu.cn)

¹State Key Laboratory of Flexible Electronics (LoFE) & Jiangsu Key Laboratory of Smart Biomaterials and Theranostic Technology, Institute of Advanced Materials (IAM), Nanjing University of Posts and Telecommunications, 210023 Nanjing, China

²College of Electronic and Optical Engineering & College of Flexible Electronics, Nanjing University of Posts and Telecommunications, 210023 Nanjing, China



unidirectional data collection through low-cost passive tags, making it ideal for logistics tracking, warehouse management, and access control.

Building upon these capabilities, NFC/RFID technologies offer distinct advantages for wearable and implantable devices that demand both miniaturization and flexibility^{19,20}. The first notable characteristic of NFC/RFID technology is its support for wireless power and data transmission²¹. NFC systems and specific RFID implementations (such as short-range applications at 13.56 MHz) employ inductive electromagnetic coupling between antennas to achieve power transfer and data communication, whereas RFID systems operating at UHF bands or intended for extended-range operation rely on far-field electromagnetic wave propagation. This wireless transmission capability of NFC/RFID systems eliminate the requirement for batteries or physical electrical connections of sensors. The second is direct sensing capabilities: NFC/RFID antennas can be modified for direct sensing, offering unique benefits by integrating data transmission and sensing modules. Thirdly, this technology ensures rapid data exchange and enhanced security. Information exchange through NFC/RFID technology typically occurs in under 0.1 seconds¹⁷, enabling rapid acquisition of patient physiological data. The secure communication protocols further protect sensitive patients' data during transmission. Last but not least is the adaptability to achieve flexibility and biocompatibility. Specific designs like serpentine structures¹⁸ and 3D helical structures²², along with materials such as silver nanowires² and MXene²³, could enhance the flexibility of NFC/RFID antennas, exerting no extra mechanical stiffness for biomedical systems. Antennas fabricated from bioabsorbable materials further enhance their suitability for implantable biomedical applications⁸.

Taken together, these advantages have drawn increasing attention to NFC/RFID systems as enabling technologies for next-generation wearable and implantable biomedical devices, spurring comprehensive reviews in this interdisciplinary field. However, existing reviews typically focus on sensor materials, design principles, sensing mechanisms, and application scenarios^{24–27}. Antennas, despite being crucial elements of wireless systems, often receive only cursory attention regarding their contributions to sensor or drug delivery functionality^{28,29}. To address this gap, our review explores the specific design requirements and working mechanisms of antennas for wearable and implantable applications. We provide a comprehensive summary and evaluation of flexible NFC/RFID-based sensors/systems (i.e., sensors/systems that utilize NFC or RFID modules for wireless communication and/or power transfer, or directly employ antenna structures as sensing elements) for medical applications (Table 1), offering valuable insights for researchers and practitioners in this field.

This review is structured as follows (Fig. 1): requirements and design mechanisms of NFC/RFID antennas in wearable and implantable contexts, recent advancements in NFC/RFID-based physical and bio/chemical sensors for physiological health monitoring, emerging NFC/RFID-based implantable drug delivery systems, and existing challenges as well as future research directions. Antenna design forms the foundation of all wireless communication in following advanced functional systems and is therefore expected to be addressed first. Physical and bio/chemical sensors represent the two major sensing paradigms that enable data collection from the human body, with distinct design considerations and applications. Finally, drug delivery systems represent the advanced intervention capabilities that complete the sensing-to-treatment pipeline. This organizational approach allows us to examine both the enabling technology (antenna designing) and their applications (sensing and therapeutic delivery) in a logical progression from fundamental components to integrated systems. By focusing on these key areas, we aim to provide a thorough analysis of current researches in this interdisciplinary field, highlighting the cooperation of antenna design with flexible materials and soft devices in advancing wearables and implants.

The requirements and design mechanisms of NFC/RFID antenna circuit

NFC/RFID-based communication systems synergistically integrate sensing and wireless power transfer through electromagnetic coupling between a reader antenna and a passive tag antenna, forming a distributed RLC resonant network where paired antennas (mostly in coil forms) establish mutual inductance.

In sensing mode, the tag antenna embeds environment-responsive components that modulate its equivalent circuit parameters (R, L or C) proportionally to external stimuli such as temperature or pressure. This parametric variation induces quantifiable resonant frequency deviations that are captured through mutual coupling by the reader antenna, and these deviations can then be demodulated into quantized sensor data.

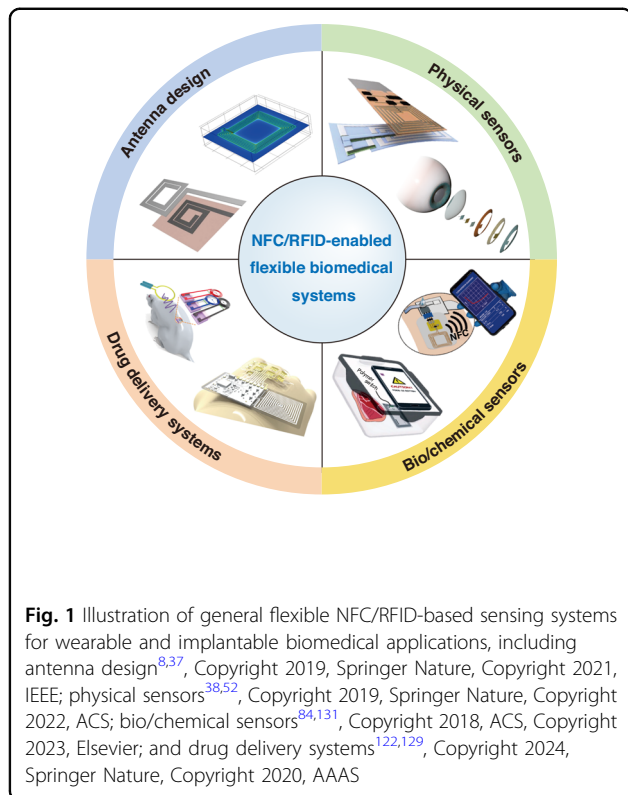
In wireless power transfer mode, optimized power transfer is achieved through mutual coupling between the reader and the tag, where the tag-integrated energy harvesting circuitry converts induced AC power into regulated DC output with dynamic impedance matching ensuring continuous energy delivery for battery-less sensors and embedded microcontrollers.

In the implantable and wearable applications of NFC/RFID antenna, not only strict performance standards need to be satisfied, but also safety and comfort issues in practical use should be considered. These challenges have led to increasing research efforts focused on optimizing NFC/RFID antenna designs for implantable and wearable

Table 1 Comparison of recent advances in NFC/RFID-based biomedical applications

System type	Working frequency	Working distance (mm)	Chip configuration	Modulation technique	Mechanical Properties	Size (mm)	Application scenario	Ref.
Physical sensors	13.56 MHz	~10	RF430FRL152H	ASK ^a	Flexible and stretchable	7 (radius)	Intraocular pressure monitoring	²
	13.56 MHz	12	Chip-free	ASK	Flexible and stretchable	51.6 × 43.2	Pulse, breath, motion analyzing	³⁸
	13.56 MHz	~300	RF430FRL152H	ASK	Flexible and stretchable	6 × 2	Pressure and temperature monitoring	¹⁵
	13.56 MHz	~15	TRF79x0ATB	ASK	Flexible	30 × 18 × 2	Pressure and temperature monitoring	⁷¹
	13.56 MHz	10	NT3H2111	ASK	Flexible	15 × 75	Calcium and chloride ions detecting	¹⁰¹
	13.56 MHz	~38	RF430FRL152H	ASK	Flexible	25 (radius)	Sweat analyzing	¹⁰⁴
	4.1 GHz	10	Chip-free	AM/FM ^b	Flexible and stretchable	~5 (radius)	Glucose/ intraocular Pressure monitoring	⁵³
	433 MHz	10	Specifically designed	ASK	Flexible	7 (radius)	Diabetic retinopathy Diagnosis and therapy	¹¹⁶
	13.56 MHz	–	NT3H2111	ASK	Flexible and stretchable	~43 × 20	Wound infection monitoring and drug delivery	¹¹⁹
	36 MHz	–	nRF52832 (BLE ^c)	GFSK ^d	Flexible	~37 × 20	Transdermal drug delivery	¹²²
Drug delivery devices	5/10/15 MHz	50	Chip-free	–	Flexible	~30 × 35	Powering for actively triggered drug delivery	¹²⁹
	12 MHz	50	Chip-free	–	Flexible	~5 (radius)	Intracellular drug delivery	¹²⁴

^aAmplitude-shift keying^bAmplitude modulation/Frequency modulation^cBluetooth low energy, in which case NFC/RFID technologies are applied to power the bluetooth module wirelessly^dGaussian frequency shift keying



applications. To this end, we will first summarize the key requirements that NFC/RFID antennas must fulfill in implantable and wearable scenarios, followed by an analysis of design strategies tailored to meet these requirements.

Specific requirements for implantable or wearable applications

The NFC/RFID-based communication system consists of a reader and a tag. NFC/RFID tag antennas significantly impact the quality of near-field communication. Given their unique operating environments, such as curved body surfaces or deep tissues *in vivo*, properties like miniaturization, high transmission efficiency, flexibility, biocompatibility and biodegradability are essential for user comfort, effective signal collection, and biosafety.

Miniaturization

Given that strict size and weight limitations are necessary for human comfort, antenna miniaturization is a consistent requirement in biomedical applications. The miniaturization of antennas is limited by the operating frequency's wavelength and energy transmission efficiency. It is known that the antenna size is proportional to its operation wavelength, and for commonly adopted NFC/RFID bands, the operation wavelengths are considerably long (For instance, the Industrial Scientific Medical band at 2.45 GHz corresponds to a free-space

wavelength of 122 mm). Although the high permittivity of human tissue can significantly reduce antenna size, it also considerably degrades transmission efficiency. Additionally, studies have shown that higher frequencies result in greater energy absorption, further reducing energy transmission efficiency. Therefore, it is essential to strike a balance between antenna miniaturization and transmission efficiency.

Coil antennas serve as the fundamental components in NFC and HF RFID systems operating at 13.56 MHz, achieving remarkable miniaturization despite the low operating frequency (free-space wavelength ~ 22 m)³⁰. This miniaturization is enabled by tightly coupled multi-turn spiral configurations, where the cumulative conductor length generates substantial distributed inductance, while the inter-turn capacitive coupling introduces effective capacitance. Through strategic optimization of turn count, conductor width, and inter-turn spacing, coil antennas achieve self-resonance at target frequencies with sub-wavelength physical dimensions. However, it should be noted that the values of inductance and capacitance would affect the power transmission efficiency between the reader and the tag as they determine the resonant characteristics and impedance matching of the system. Therefore, miniaturization and transmission efficiency should be balanced adequately during the design³¹.

Transmission efficiency

The NFC antennas are usually used to realize data exchange from different devices, or energy transmission to power sensors and electronic circuits. Thus, to ensure the transmission quality, the high transmission efficiency of NFC antennas is essential. Typically, NFC antennas can achieve a transmission efficiency of 70-90% through inductive coupling technology, and the efficiency decreases when the separation distance between two antennas increases. It should be noted that there are two factors that would affect the antenna efficiency: the properties of the conductor and substrate, and the alignment between the two NFC antennas. For the former, materials with higher conductivity and substrates with lower loss tangents are preferred to achieve high transmission efficiency. However, while traditional structures based on copper and solid PCBs exhibit low loss characteristics, they often fail to meet the requirements for flexibility and stretchability. Regarding the latter, optimal efficiency is achieved only when two NFC antennas are positioned parallel with their axes precisely aligned^{32,33}. Any deviation from this alignment can lead to substantial variations in the mutual inductance coefficient, thereby negatively impacting transmission efficiency. Since achieving perfect alignment is often impractical, recent advancements have focused on mitigating this limitation. For instance, ferrite-backed

antennas have been adopted to broaden the magnetic field distribution, thereby enhancing radiation efficiency³⁴. Additionally, integrating rectifiers with supercapacitors has been explored to achieve a synergistic balance between energy storage and transmission. Despite these solutions, maintaining high efficiency in realistic scenarios still remains a challenge³⁵.

Flexibility/stretchability

Traditional commercial NFC tag antennas, such as NFC coils, are typically established on a rigid PCBs etched with copper³⁶, with rigid sensors and hard electronic components integrated on them. However, these rigid designs lack flexibility and could cause discomfort for the human body. More importantly, they are susceptible to fractures, which limits the application of NFC-based wearable sensor devices. Therefore, there is a preference for stretchable sensors and flexible electronic components constructed from materials like PDMS, PET, and other intrinsically flexible materials. For instance, PDMS is employed in the fabrication of smart wound dressings capable of continuous temperature monitoring³⁷, while SEBS-based stretchable sensors can be seamlessly integrated with human skin to acquire both physiological parameters and motion-related signals³⁸. These materials are chosen for their ease of bending, excellent electromagnetic properties, and high thermal and chemical stability. Alternatively, stretchable liquid conductors like Eutectic Gallium Indium (EGaIn) are adopted to replace traditional copper conductors. However, the high cost of these liquid conductors limits their suitability for large-scale manufacturing³⁹. Additionally, the interface between rigid electronic components and stretchable materials tends to be relatively weak, and fully flexible electronic components have not yet been developed³⁸. Thus, achieving a completely soft, comfortable, and stretchable NFC-based sensor system remains a major challenge.

Material biocompatibility/biodegradability

For NFC/RFID-based implantable sensors exposed to human tissues, the biocompatibility and biodegradability of the materials are crucial considerations. Biocompatible materials can be in direct contact with human tissues without eliciting an immune response³⁹, which ensures no occurrence of significant adverse reactions and maintains patient safety. While biodegradable materials can be absorbed or excreted by the human body under natural or chemically induced conditions once the operational lifespan of the implanted devices concludes⁴⁰. This characteristic eliminates the need for secondary surgery to remove the devices, thereby reducing potential risks to patients.

Antenna as a sensing element

It is known that antennas can be regarded as LC resonators and their resonant performance—resonant frequencies, reflection coefficient, and input impedance—varies with changes in structure parameters as well as the working environment. Consequently, antennas can be utilized as the sensor elements, with their performance reflecting variations in the target. Unlike systems that merely use NFC/RFID technology for sensor data transmission, those equipped with NFC/RFID-based antenna sensors utilize the antenna itself as the sensing element, which enables higher integration and miniaturization. Currently, antennas adopted as sensors can be separated into two categories: microstrip patch antenna sensors and passive LC resonant sensors.

Microstrip patch antenna sensor

Figure 2a illustrates a typical microstrip patch antenna designed for far field radiation, consisting of three components, a rectangular metal patch on the top, a metal ground at bottom and a dielectric substrate in between⁴¹. The thickness of the substrate (h) is much smaller than the free-space wavelength (λ_0), typically in the range of $0.003\lambda_0$ to $0.05\lambda_0$. For a rectangular patch, its length L is usually within the range $\lambda_0/3 < L < \lambda_0/2$, and the typical electric field lines are shown in Fig. 2b. As can be seen, most of the electric field lines are concentrated within the substrate, with only a few extending into the air. When $W/h \gg 1$, the electric field lines are primarily confined to the substrate. The fringing effect causes the microstrip patch to appear electrically larger than its physical dimensions. As demonstrated in Fig. 2c, a rectangular microstrip patch antenna can be modeled as an array of two narrow radiating slots, each with width W and height h , separated by a distance L . Basically, the transmission-line model represents the microstrip antenna as two slots separated by a low-impedance transmission line of length L .

Due to edge effects, the electrical length of the patch exceeds its physical length L , necessitating a compensation length ΔL to accurately calculate its resonant frequency:

$$\Delta L = 0.412h \frac{(\epsilon_e + 0.3)(\frac{W}{h} + 0.264)}{(\epsilon_e - 0.258)(\frac{W}{h} + 0.8)} \quad (2-1)$$

$$\epsilon_e = \frac{\epsilon_r + 1}{2} + \frac{\epsilon_r - 1}{2} \left(1 + 12 \frac{h}{W} \right)^{-\frac{1}{2}} \quad (2-2)$$

where ϵ_r and ϵ_e are the relative and effective dielectric constants of the dielectric substrate, respectively, h denotes the substrate height, and W indicates the width of the rectangular patch. Consequently, the relationship between the patch dimensions and the required resonant

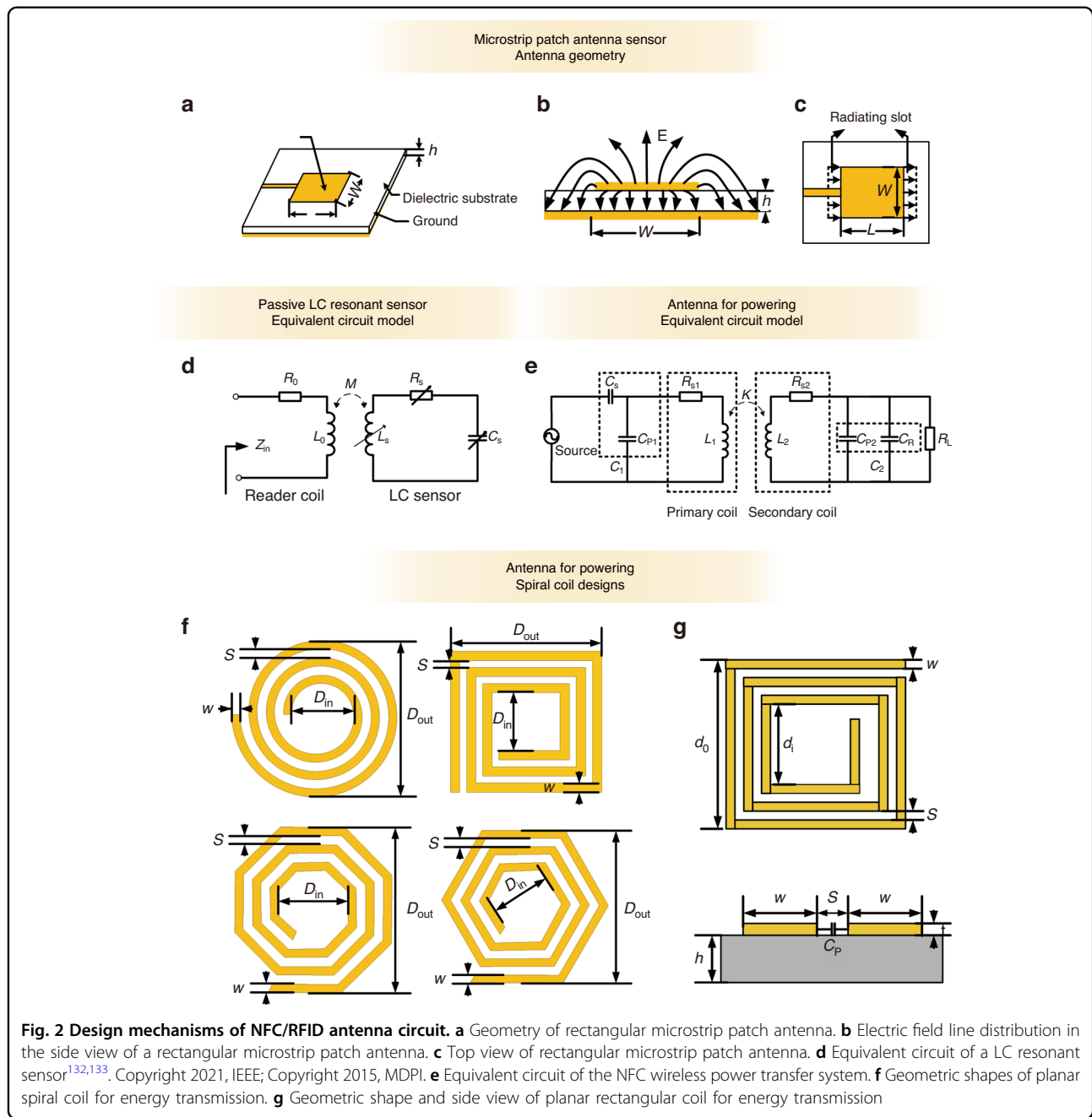


Fig. 2 Design mechanisms of NFC/RFID antenna circuit. **a** Geometry of rectangular microstrip patch antenna. **b** Electric field line distribution in the side view of a rectangular microstrip patch antenna. **c** Top view of rectangular microstrip patch antenna. **d** Equivalent circuit of a LC resonant sensor^[32,133]. Copyright 2021, IEEE; Copyright 2015, MDPI. **e** Equivalent circuit of the NFC wireless power transfer system. **f** Geometric shapes of planar spiral coil for energy transmission. **g** Geometric shape and side view of planar rectangular coil for energy transmission

frequency f can be expressed as

$$L = \frac{c}{2f\sqrt{\epsilon_e}} - 2\Delta L \quad (2-3)$$

$$W = \frac{c}{2f} \left(\frac{\epsilon_r + 1}{2} \right)^{-\frac{1}{2}} \quad (2-4)$$

where c is the speed of light.

It can be concluded from these equations that the resonant frequency f of the antenna sensor is affected by the

dimensions of the rectangular microstrip patch (W and L) and the properties of the dielectric substrate (h and ϵ_r). Thus, various sensors have been developed accordingly. For instance, a passive wireless strain sensor based on microstrip patch antenna has been proposed, where shifts in resonant frequency occur in response to the patch's deformation^[42]. Moreover, a frequency-agile microstrip patch antenna has been established on a ferroelectric substrate composed of barium strontium titanate ($Ba_xSr_{1-x}TiO_3$), achieving frequency agility through alterations in the dielectric constant of the substrate^[43].

Passive LC resonant sensor

As illustrated in Fig. 2d, a typical *LC* resonant passive sensor can be modeled as a serial LCR resonant circuit, which consists of three fundamental components, inductors (L_s), capacitors (C_s), and parasitic resistors (R_s). These elements collectively determine the resonant characteristics of the sensor, where its resonant frequency (f_s) and quality factor (Q_s) can be calculated as:

$$f_s = \frac{1}{2\pi\sqrt{L_s C_s}} \quad (2-5)$$

$$Q_s = \frac{1}{R_s} \sqrt{\frac{L_s}{C_s}} \quad (2-6)$$

It can be concluded from Eqs. (2-5) and (2-6) that f_s and Q_s are directly influenced by L_s , C_s and R_s . Consequently, R_s , L_s and C_s can serve as sensitive components for *LC* sensors, with Z_s representing its equivalent input impedance.

The reading coil can be equivalent to an inductor (L_0) and a parasitic resistor (R_0), and the coupling strength between the sensor inductors L_s and reader inductor L_0 is represented by M . Therefore, the equivalent input impedance for a reading coil coupled with an *LC* sensor can be written as:

$$Z_{in} = R_0 + j\omega L_0 + Z_s \quad (2-7)$$

Substituting equations (2-5) and (2-6) into equation (2-7), the real part of Z_{in} can be derived as

$$Re(Z_{in}) = R_0 + 2\pi f L_0 k^2 Q_s \frac{f/f_s}{1 + Q_s^2(f/f_s - f_s/f)^2} \quad (2-8)$$

Equation (2-6) reveals that R_s is inversely proportional to Q_s of the *LC* sensor, such that any variation in R_s leads to changes in the amplitude of $Re(Z_{in})$ as indicated by equation (2-8). These changes can be detected by external devices. Besides, if Q_s is sufficiently large such that $1/(4Q_s^2) \ll 1$, then f_s approximates $f = f_{Re-max}$ with a maximum $Re(Z_{in})$ according to equation (2-8), which implies that variations in L_s and C_s can be directly observed by monitoring changes in f_{Re-max} .

In addition, Z_{in} can be converted to the reflection coefficient (S_{11}) according to the following expression:

$$S_{11} = \left. \frac{Z_{in} - Z_0}{Z_{in} + Z_0} \right|_{Z_0=50\Omega} \quad (2-9)$$

where $Z_0 = 50 \Omega$ represents the characteristic impedance of the feed. In this case, variations in R_s , L_s and C_s can also

be detected by observing the S_{11} curve of the reading coil, which can be obtained with a Vector Network Analyzer (VNA).

Based on the above theory, various sensors have been developed^{44,45}. For instance, Sridhar et al. introduced a hydrogel pH sensor based on *LC* resonant circuit⁴⁴. Changes in pH values alter the dimensions of the hydrogel elements, leading to the variation of L_s and resulting in a frequency shift in the, which can be detected by monitoring the frequency shift of S_{11} . Ren et al. describes the design of an *LC* resonant passive sensor for relative humidity and temperature monitoring⁴⁵. In this design, environmental humidity affects the capacitance, leading to the change in the resonant frequency, while ambient temperature influences the resistance, thereby altering the quality factor. Consequently, by measuring the $Re(Z_{in})$ of the reading coil, variations in ambient temperature and relative humidity can be accurately recorded.

Antenna for powering

In addition to *LC* sensors, magnetic coupling can be utilized in NFC systems consisting of two coils, where energy is transferred from the primary to the secondary coil, realizing power transmission in near field. When excluding the integrated circuit (IC) components, the equivalent circuit of NFC system can be simplified as depicted in Fig. 2e, where the mutual inductance between the two coils can be equivalent to a magnetic coupling transformer with a coupling coefficient K . In this circuit, the primary coil antenna is matched with the voltage source through the capacitor C_s . The resistor R_{s1} and R_{s2} accounts for the losses in the primary and secondary coil antennas, respectively. Inductor L_1 and L_2 serve as series resistors. The capacitors C_{p1} and C_{p2} represent the parasitic capacitances of the primary and secondary coils, while C_R is the tuning capacitor for optimal impedance matching, and R_L represents the load.

The design of planar spiral antennas varies depending on application requirements. While planar spiral antennas can adopt diverse geometries (including circular, rectangular, and polygonal configurations), each structure exhibits distinct electromagnetic characteristics, as shown in Fig. 2f, g. Circular coils leverage rotational symmetry to achieve uniform magnetic flux distribution and minimize edge effects, with key parameters such as the radius of curvature and angular alignment directly influencing their quality factor and coupling efficiency. Conventional polygonal coils, such as hexagonal designs, feature seamless tiling and flexible modularity, optimizing performance in irregular layouts and maximizing anti-misalignment characteristics. The number of sides and symmetry of polygonal coils critically affect their

performance. In contrast, rectangular or square coils provide a larger effective coupling area compared to circular or elliptical counterparts with equivalent horizontal and vertical dimensions, owing to their orthogonal symmetry and maximized edge utilization. This rectangular coil consists of a metal coil on top and a substrate below, where the outer and inner diameters of the coil are denoted as d_0 and d_i , respectively, w and s are the width of each coil wires and their separation space. Due to its predictable field confinement, fabrication simplicity, and compatibility with standard planar manufacturing processes, it is widely employed in wireless communication, NFC/RFID, and electromagnetic induction systems.

The key factors influencing transmission characteristics include the coupling coefficient K , coil inductance L and quality factor Q ⁴⁶, which are expressed as follows⁴⁷:

$$L = \frac{1.27 \times \mu_0 n^2 d_{avg}}{2} \left[\ln\left(\frac{2.07}{\phi}\right) + 0.18\phi + 0.13\phi^2 \right] \quad (2 - 10)$$

$$K = \frac{M}{\sqrt{L_1 L_2}} \text{ with } M = g \sum_{i=1}^{n_1} \sum_{j=1}^{n_2} M_{ij}(r_i, r_j, D) \quad (2 - 11)$$

$$Q \approx \frac{\omega L}{R_s} \text{ for small } C_p \text{ or low } f \quad (2 - 12)$$

where $d_{avg} = (d_0 + d_i)/2$ represents the average radius, $\phi = (d_0 - d_i)/(d_0 + d_i)$ represents the fill factor, and $\mu_0 = 4\pi \times 10^{-7} H/m$ represents the vacuum permeability. The coupling inductance M and the number of coils turns, denoted n_1 and n_2 for the primary and secondary coils, respectively, also influence the system's performance. Besides, r_i and r_j refer to the radius of the i th and j th coil turns of the primary and secondary coils, respectively, and D represents the distance between the two coils. The constant g is specific to the shape of a planar spiral coil (PSC), with $g = 1.1$ for square-shaped PSCs. The angular frequency $\omega = 2\pi f$ defines the system's operational frequency.

When both coils are tuned to the operating angular frequency, such that $\omega = 1/(C_1 L_1)^{1/2} = 1/(C_2 L_2)^{1/2}$, maximum transmission efficiency can be achieved⁴⁷:

$$\eta = \frac{K^2 Q_1 Q_L}{1 + K^2 Q_1 Q_L} \cdot \frac{Q_L}{Q_2 + Q_L} \quad (2 - 13)$$

where Q_1 and Q_2 represent the quality factors of the primary and secondary coil antennas, respectively, and Q_L represents the loaded quality factor of the secondary coil

at resonance, which can be expressed as:

$$Q_L = \frac{1}{R_{s2}/\omega L_2 + \omega L_2/R_L} = \frac{1}{R_{s2} \cdot \sqrt{C_2/L_2} + 1/R_L \cdot \sqrt{L_2/C_2}} \quad (2 - 14)$$

where C_2 can be represented as $C_2 = C_{p2} || C_R$.

Based on the discussions above, it can be concluded that sensor performance can be reflected on the frequency shift of the antenna, which is caused by variations in its equivalent inductance, capacitance, or resistance. These variations are achieved by incorporating sensitive elements into the antenna structures, consequently changing the dielectric properties of the substrate, changing the dimensions of the antenna, or introducing inductive and capacitive loadings. To maximize transmission and power transfer efficiency in NFC coils, careful attention must be given to the coil's dimensions, optimizing inductance, capacitance, and resistance for resonant frequency and impedance matching. Additionally, proper alignment and placement are crucial; the primary and secondary coils must be axially aligned and kept at an optimal distance. Any axial misalignment or distance variation significantly reduces transmission efficiency between the coils.

NFC/RFID-based flexible physical sensors

The NFC/RFID-based sensor systems can be broadly categorized into physical sensors and biological/chemical sensors, depending on their sensing principles and application scenarios. This section provides a comprehensive exploration of strategies and approaches for incorporating NFC/RFID antennas into wearable or implantable physical sensing systems, covering single to multiple physical quantities monitoring both in vitro and in vivo. Specific focus is given to wearable strain sensors, wearable multimodal sensors, and implantable sensors.

Wearable strain sensors

Strain sensing plays a vital role in physiological monitoring, with applications ranging from respiratory tracking to pulse wave monitoring, offering opportunities for continuous and noninvasive health assessment. One notable application is in the detection of intraocular pressure (IOP), a critical parameter in the management of glaucoma, which is the second leading cause of blindness worldwide, following cataracts⁴⁸. Traditionally, IOP measurement is performed using a Goldman applanation tonometer, a standard medical device that requires the expertise of medical professionals and limits patient monitoring to specific times and locations. Additionally, this method necessitates the use of anesthesia, further complicating the procedures.

Currently, smart contact lenses equipped with NFC/RFID antennas have been reported as IOP sensors. These

devices incorporate a NFC/RFID coil within a flexible lens, facilitating wireless, real-time IOP monitoring—thus offering a more practical and convenient alternative to wired smart lenses⁴⁹. A key innovation in these devices is the hybrid rigid-flexible structural design, which enhances sensitivity by concentrating strain in the flexible component⁵⁰. Strain sensors in these smart contact lenses are generally categorized as either resistive or capacitive. As IOP increases, the resistance in resistive sensors rises, leading to a linear shift of the S_{11} value at the resonant frequency (Fig. 3a)⁵¹. In contrast, capacitive strain sensors detect corneal dilation caused by increased IOP through changes in the capacitor's shape, thus enabling wireless IOP monitoring via resonant frequency changes induced by capacitance variations. For instance, Fig. 3b depicts a capacitive contact lens-based sensing system that utilizes a pyramidal microstructure to enhance pressure sensitivity⁵². This system leverages capacitive sensing and a dielectric elastomer to detect corneal dilation from elevated IOP. An external coil connected to a VNA reads the S_{11} value to track IOP readings, with readers integrated into the glasses frame for simplified wireless data acquisition.

Moreover, contemporary smart contact lenses are trending towards multifunctionality. Figure 3c shows a multiplex system capable of simultaneously detecting tear glucose concentration and IOP. In this system, elevated IOP changes corneal curvature, compressing the dielectric to decrease its thickness and increase system capacitance. Concurrently, the biaxial lateral expansion of the helical coil increases inductance, thus affecting the resonant frequency of the system. The glucose sensor, operating as a resistive element, also influences the S_{11} value, effectively avoiding signal conflicts⁵³. Another innovative system integrates an NFC chip with a temperature sensor and uses EGaIn for connections, allowing for IOP and temperature detection with just a smartphone equipped with NFC capabilities², thus greatly simplifying sensor data acquisition and processing (Fig. 3d).

For personalized medicine, mere detection is insufficient; targeted treatment tailored to individual conditions is more beneficial. Such demands have catalyzed a novel class of smart contact lenses integrates a dosing component⁶, allowing for *in situ* IOP detection and on-demand medication delivery. In another case, Fig. 3e showcases a highly integrated diagnostic and therapeutic contact lens that combines a chip and a drug delivery system for wireless IOP monitoring and management⁵⁴, which could hopefully improve glaucoma treatment.

Beyond localized strain sensing such as IOP monitoring, strain sensors are also widely employed to detect dynamic body motions, including joint flexion, muscle contraction, and respiration, offering valuable insights into a broad range of physiological activities. However, many of these

devices still depend on wired connections for signal transmission^{55–58}. To address this, wireless strain sensing systems based on NFC/RFID technology have been developed. For instance, the system illustrated in Fig. 4a employs a $Ti_3C_2T_x$ MXene strain-sensitive resistor, supported by an NFC smartphone for wireless power supply, signal transmission and reception, making it particularly suitable for electronic skin applications aimed at monitoring finger, palm, or sole movements⁵⁹. In addition to skin-mounted sensors, wireless strain sensors have also been integrated into clothing as electronic textiles for detecting human motion. Figure 4b showcases a strain sensor made from reduced graphene oxide (rGO)-dyed wool fabric. This sensor, produced through embroidery techniques, seamlessly integrates with a textile-based NFC antenna to enable wireless strain sensing of finger bending⁶⁰.

Furthermore, advancements in medical monitoring technology have necessitated comprehensive whole-body movement monitoring, beyond localized areas. This requirement calls for a body area sensing network capable of monitoring multiple body parts. NFC/RFID technology offers a solution by enabling the creation of an extensive network of strain sensors. Such a network is typically composed of multiple NFC sensor nodes that communicate through several partially overlapping flexible planar magnetic resonators (flexible planar coils) (Fig. 4c)⁶¹. These sensor nodes can be integrated into clothing, with an external reader providing both power and data transmission. As shown in Fig. 4d, the sensor nodes attach directly to the skin, while the wiring is embedded in the clothing fabric. When the reader approaches one coil, it activates all sensor nodes and receives their signals⁶², thus simplifying the overall configuration and reducing wiring complexity.

Simplification of sensor node design is also a critical aspect of improving these systems. Bao et al. have developed sensor nodes that consist only of an antenna and a resistive strain sensor, promoting system miniaturization and flexibility³⁸ (Fig. 4e, f). An RFID-based external reader can detect changes in the S_{11} value of the tag in response to strain, facilitating comprehensive monitoring of human physiological activities. Figure 4g shows another design which features a high-frequency tension diode for rectification and includes an electrochromic display (ECD) pixel⁶³. When the current in the ECD pixel exceeds a specific threshold, a distinctive blue color appears, visually indicating strain on the human body. This visual cue simplifies the interpretation of strain data, providing a straightforward method for assessing physiological conditions.

Wearable multimodal sensors

In the realm of personalized medicine and the rapidly advancing field of wearable biomedical sensors, the

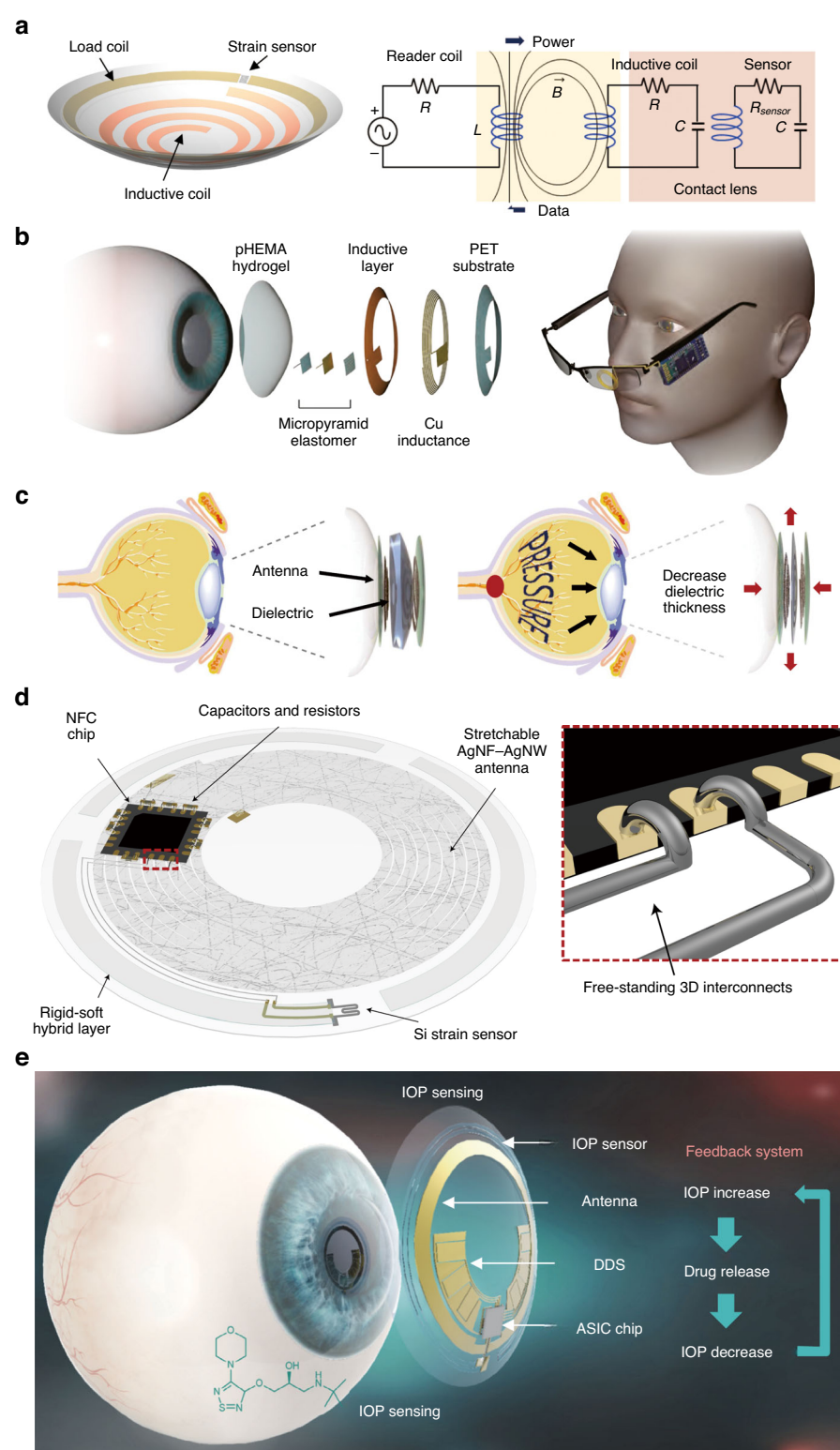


Fig. 3 A variety of NFC/RFID-based contact lens designs with the ability to monitor IOP. **a** Schematic illustration of the resistive wireless IOP sensing contact lens, and the equivalent circuit diagram⁵¹. Copyright 2020, ACS. **b** Schematic diagram of the capacitive smart contact lens and the reader integrated in the glasses⁵². Copyright 2022, ACS. **c** Schematic illustration of the mechanism by which an overall flexible contact lens measures IOP⁵³. Copyright 2017, Springer Nature. **d** Schematic illustration of the contact lens integration system with the introduction of NFC chip, the enlarged part is schematic illustration of the printed free-standing 3D interconnects on the metallic pads of an NFC chip². Copyright 2021, Springer Nature. **e** Closed-loop smart contact lens integrated with a flexible drug delivery system and a microchip, which are designed for the monitoring and control of IOP⁵⁴. Copyright 2022, Springer Nature



detection of isolated physical quantities often proves inadequate for comprehensive patient care. There is a pressing need for wearable medical sensors capable of simultaneously monitoring multiple physiological

parameters, thus enabling a more detailed analysis of patient health⁶⁴. For instance, temperature is a crucial indicator of inflammation, infection, and wound healing potential⁶⁵, while skin strain is an effective metric for

evaluating wound closure and tissue expansion during the healing process⁶⁶. Consequently, a sensor system that simultaneously tracks temperature and strain would significantly enhance wound care and management (Fig. 5a)³⁷. The smart bandage features a highly sensitive strain sensor that utilizes a Poly(3,4-ethylenedioxythiophene) polystyrene sulfonate (PEDOT:PSS) microfluidic channel embedded in a PDMS substrate. The resistance of the strain sensor increases as the microchannel expands in response to applied strain. Additionally, the temperature sensor utilizes the thermosensitivity of PEDOT:PSS, where an increase in temperature enhances carrier mobility, leading to a decrease in resistance.

In addition to wound management, multimodal sensors are also effectively monitoring pressure injuries. For hemiplegic patients, areas around bone protrusions can rapidly heat up under constant pressure, which can lead to severe pain, functional impairment, skin breakage, and other complications. A specialized device designed to fit the contours of bone prominences includes an NFC System-on-Chip(SoC) and a coil antenna connected to pressure and temperature sensors via serpentine wires (Fig. 5b)¹⁵. PDMS encapsulation ensures environmental isolation, electronic protection, and fluid buffering, enhancing the durability and reliability of the sensor. Extending this concept further, Fig. 5c demonstrates a Galvanic Skin Response (GSR) sensor, which builds upon the previous design of Fig. 5b and is capable of measuring pressure, temperature and hydration levels at joint sites to accurately assess pressure damage. Such sensors can be strategically distributed across various body parts forming a comprehensive full-body sensing network. The network, controlled by a multiplexer and an NFC reader, communicates with primary antennas located on the wheelchair (Fig. 5d)⁶⁷. This setup wirelessly powers all sensors attached to the patient and rapidly reads data from different locations using an NFC-based sequential read protocol, thus providing real-time pressure, temperature, and hydration measurements for each sensor node. The deployment of wireless sensor arrays in areas vulnerable to pressure damage allows for continuous multi-point mapping of pressure and temperature distributions (Fig. 5e)⁶⁸, offering a more comprehensive understanding and prevention of pressure injuries compared to single-point detection methods⁶⁹.

In contrast to the aforementioned systems, the configuration shown in Fig. 5f exhibits a higher degree of miniaturization and integration, enabling broad coverage and comprehensive data collection for both temperature and pressure. Furthermore, this data can be converted into thermograms and pressure maps⁷⁰, offering a visual representation of the wearer's physiological conditions. Additionally, the multimodal sensing of temperature and pressure can be extended to

prosthetics to monitor pressure injuries at amputation sites (Fig. 5g)⁷¹.

Implantable sensors

Implantable sensors are essential for capturing critical signals that are not accessible through wearable devices, such as intracranial parameters⁷² and arterial blood flow. For instance, NFC-based implantable sensors have been designed for real-time monitoring of brain oxygen saturation in mice (Fig. 6a) allows for awake-state measurements due to its compact size and biocompatible encapsulation^{73,74}. Unlike stent-based wireless blood flow sensors^{75,76} and wireless pacemakers⁷⁷, these implantable sensors allows for continuous monitoring of vascular pressure, flow rate, and temperature within blood vessels through only a minimally invasive sensing module (Fig. 6b, c)³.

Despite the reduced invasiveness, there remain concerns regarding potential tissue damage during and after implantation. Moreover, the use of non-biodegradable materials and electronic components complicates post-implantation management, often necessitating additional surgeries for removal. Addressing these issues, a fully implantable NFC sensor designed for monitoring brain temperature and pressure in mice incorporates bioabsorbable elements, such as magnesium coils, electrodes, interconnections, and silicon resistors, which dissolve within 14 days post-implantation (Fig. 6d)⁷⁸. Although the NFC chip itself remains non-biodegradable, this design significantly reduces long-term biocompatibility concerns.

For complete bio-absorbability, sensors devoid of electronic chips present a promising solution. As depicted in Fig. 6e, chip-free implantable RFID biosensors facilitate wireless passive monitoring of arterial blood flow, which is crucial for postoperative recovery⁸. These sensors detect changes in vessel diameter caused by arterial pulsation by monitoring variations in the resonant frequency of the sensor's LCR circuit. Such changes can be wirelessly detected by an external coil near the implantation site, thus providing continuous blood flow data without the need for invasive retrieval procedures. The use of bioabsorbable materials and a chip-free design eliminates the need for secondary surgeries, thereby enhancing patient safety and comfort.

Diagnostic and therapeutic integrated implantable sensors further extend their utility far beyond conventional detection by incorporating advanced treatment capabilities. Two notable examples illustrate this progress. Figure 6f shows a sensing system designed for cardiac defibrillation research⁷⁹, which not only monitors ECG signals but also features optical pacing functionality. This dual capability enables precise regulation of cardiac activity, facilitating more effective therapeutic interventions. Moreover, researchers reported an implantable

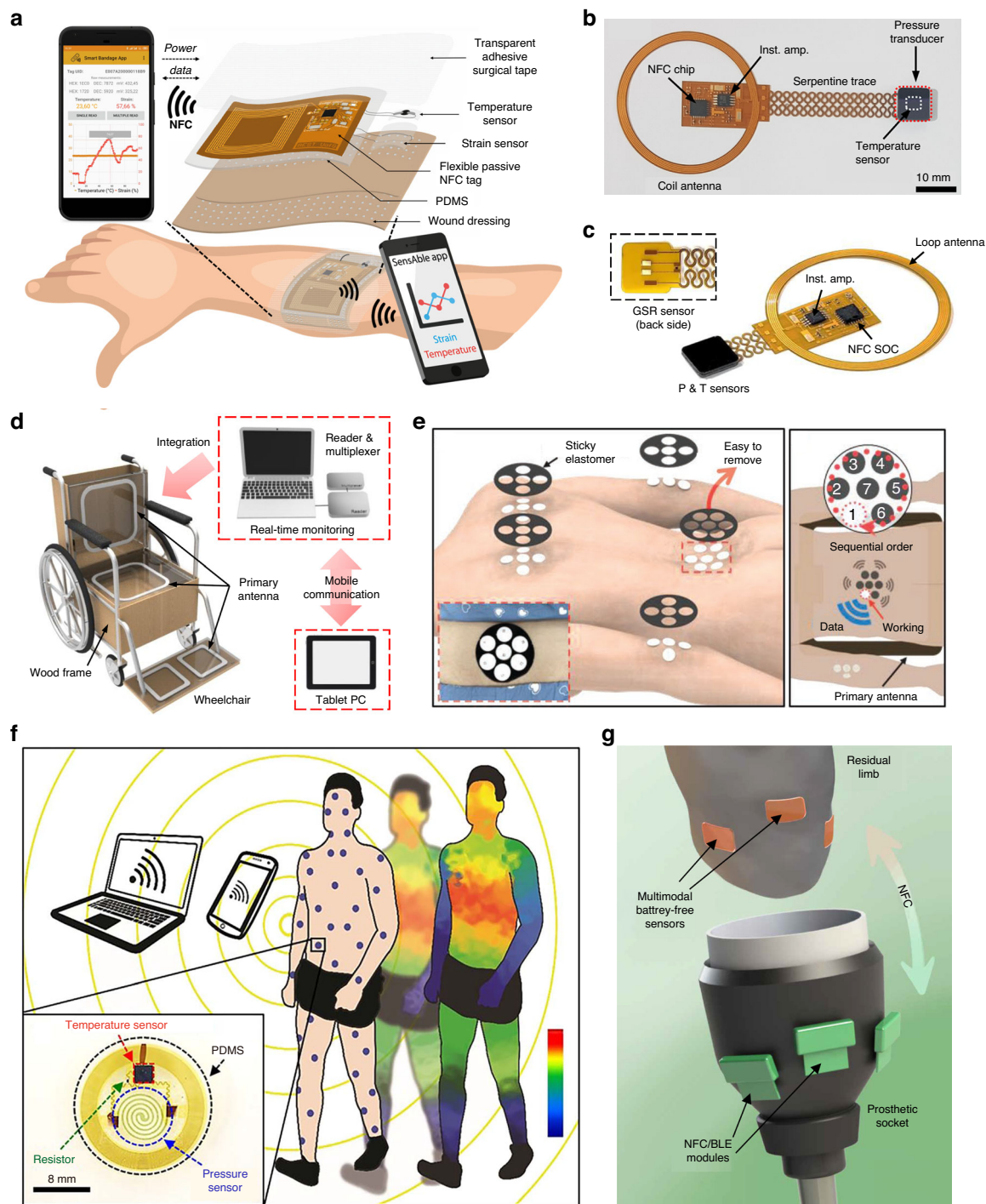
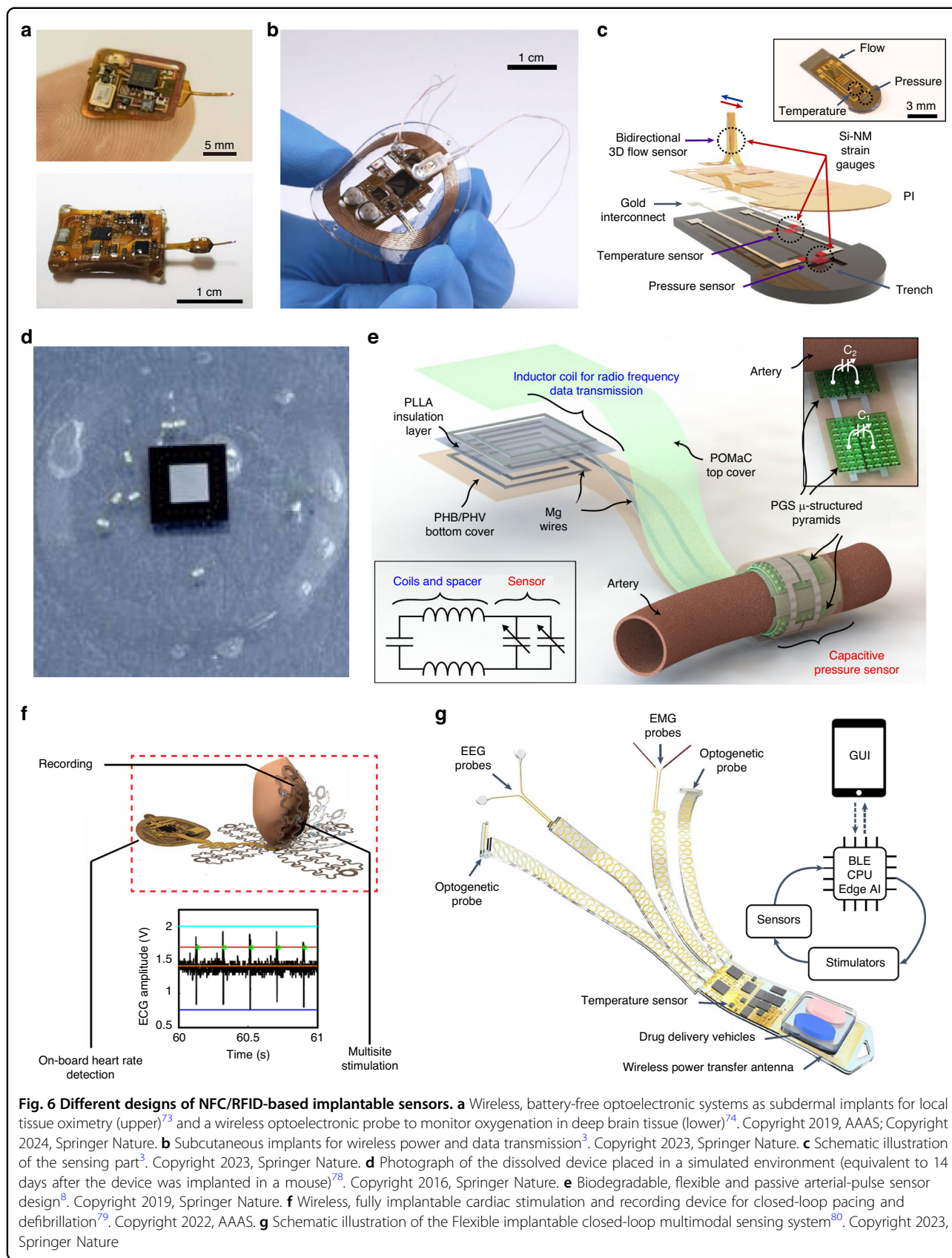


Fig. 5 Flexible wearable NFC/RFID-based sensors that can monitor multiple physical quantities. **a** The NFC-based smart bandage for wireless strain and temperature real-time monitoring³⁷. Copyright 2021, IEEE. **b** A photograph of the flexible sensor that monitors the temperature and pressure at the bony prominence before encapsulation¹⁵. Copyright 2021, Springer Nature. **c** Photograph of the battery-free, wireless sensing platform that includes crack-activated pressure sensor, temperature sensor, and GSR sensor. Inset shows the GSR sensor located at the back side of flexible PCB⁶⁷. Copyright 2023, Springer Nature. **d** Schematic illustration of the overall system integrated with a wheelchair⁶⁷. Copyright 2023, Springer Nature. **e** Sensor arrays that can continuous monitoring and mapping of pressure and temperature distribution⁶⁸. Copyright 2023, Wiley-VCH. **f** A group of thin and comfortable wireless temperature and pressure sensor systems distributed throughout the body, the enlarged part is the individual sensor section structure⁷⁰. Copyright 2018, AAAS. **g** Illustration of wireless, battery-free multimodal sensors on a residual limb and NFC/BLE modules on the outer surface of a prosthetic socket⁷¹. Copyright 2020, AAAS.



system that integrates both diagnostic and therapeutic functionalities (Fig. 6g), capable of simultaneously multiplex diagnostic (EEG, EMG, and body temperature recording) as well as combined therapeutic (neural modulation through optogenetic electrodes and drug delivery⁸⁰). The system operates autonomously in a closed-loop manner, powered by integrated artificial intelligence. The advancement of implantable sensors that combine diagnostic and therapeutic capabilities represents a significant leap forward in medical technology, promising to transform patient care through more precise and responsive interventions.

NFC/RFID-based flexible bio/chemical sensors

Biomarkers in exhaled gas and biofluid are crucial for early disease diagnosis and health monitoring. The process of detecting these biomarkers typically involves chemical reactions, necessitating more complex electronic systems for signal transmission compared to physical sensors. Integrating NFC/RFID technology with flexible biological and chemical sensors addresses these challenges by enabling miniaturization and facilitating more convenient data acquisition compared to traditional sensing systems. This section reviews the advancements in flexible gas sensors for environmental monitoring, food safety, and breath analysis as well as biological fluid sensing systems for detecting biomarkers in sweat, interstitial fluid, and tears.

Gas sensors

Gas sensing using NFC/RFID technologies for wearable/implantable biomedical applications remains an emerging field^{5,81}, while significant advancements in environmental^{81,82} and food safety monitoring^{83,84} have demonstrated the feasibility and versatility of NFC/RFID-based gas sensors. These applications are closely related to human health—exposure to harmful gases in the environment or consumption of spoiled food can pose serious risks—and are particularly relevant for healthcare personnel, industrial workers, and consumers who require real-time access to safety information. Therefore, existing systems in these domains offer valuable design insights for future development of wearable and implantable biomedical gas sensors.

In environmental gas monitoring, detecting toxic gases such as ammonia is critical not only for public safety but also for occupational health. Traditional ammonia sensors often require high operating temperatures^{81,82}, while recent advancements have led to the development of highly sensitive ammonia sensors capable of functioning at room temperature^{85–87}. Although these sensors can be integrated into wearable smart bracelets, they still depend on external power supplies and contain rigid components that limit their miniaturization and flexibility. To address

these limitations, flexible NFC antennas offer a promising solution. For example, the ammonia sensor using a wireless and passive NFC tag shown in Fig. 7a integrates a resistive sensor that is sensitive to ammonia⁸⁸. This sensor can be read using a smartphone, displaying an “on” state when the concentration is below the threshold. As the surrounding ammonia gas concentration exceeds the threshold, the circuit resistance rises (within 1 min of exposure to 35 ppm NH₃, ΔRs = 5.3 ± 0.7 kΩ), causing the chip to switch from active state to inactive state, resulting in an “off” state, thereby enabling wireless semi-quantitative detection of ammonia. Furthermore, this approach has been extended to detect other gases by assembling an array of NFC tags with different threshold resistances⁸⁹, allowing for binary-coded detection of ethanol gas concentrations from 1 ppm to 5 ppm.

Food safety, with direct implications for human health, is another critical area where gas sensors are employed to detect spoilage-related gases. Oxygen is a key factor in food spoilage and can be detected by NFC tag sensors embedded within food packaging⁸³. Additionally, biogenic amines and ammonia released during the spoilage of food, particularly meats, are also key indicators that can be monitored using NFC tag sensors (Fig. 7b)⁸⁴. In another design, tag sensors integrate four distinct sensing membranes, enabling the detection of multiple gas concentrations as well as temperature and humidity levels within the packaging. Each membrane elicits an optical response (luminescence or colorimetric change) to the target gas, with the results captured by a color detector. The test results of target gas concentrations are then intuitively transmitted to a smartphone for real-time acquisition via the NFC antenna⁹⁰ (Fig. 7c).

In clinical settings, monitoring exhaled gases is crucial for early disease diagnosis. For instance, elevated ammonia levels in breath are indicative of kidney disease^{91,92}. Moreover, rebreathing of carbon dioxide trapped in masks can negatively impact the human body. While current wearable sensors can detect ammonia in exhaled air^{85,93}, they often require external power modules, limiting their practicality. To overcome this, NFC modules have been applied to wearable smart gas sensing devices. Figure 7d shows a smart mask featuring a flexible NFC tag integrated with a photochemical sensor, which non-invasively measures the carbon dioxide concentration inside the mask⁵. The sensor and electronic components are mounted on a flexible substrate and are powered and communicate wirelessly via NFC technology, thereby enhancing the mask’s flexibility and integration capabilities.

In addition to gaseous molecules, aerosols—airborne particles that may carry pathogens—are also of significant biomedical relevance. The detection of aerosols shares similar device design principles with gas sensing,

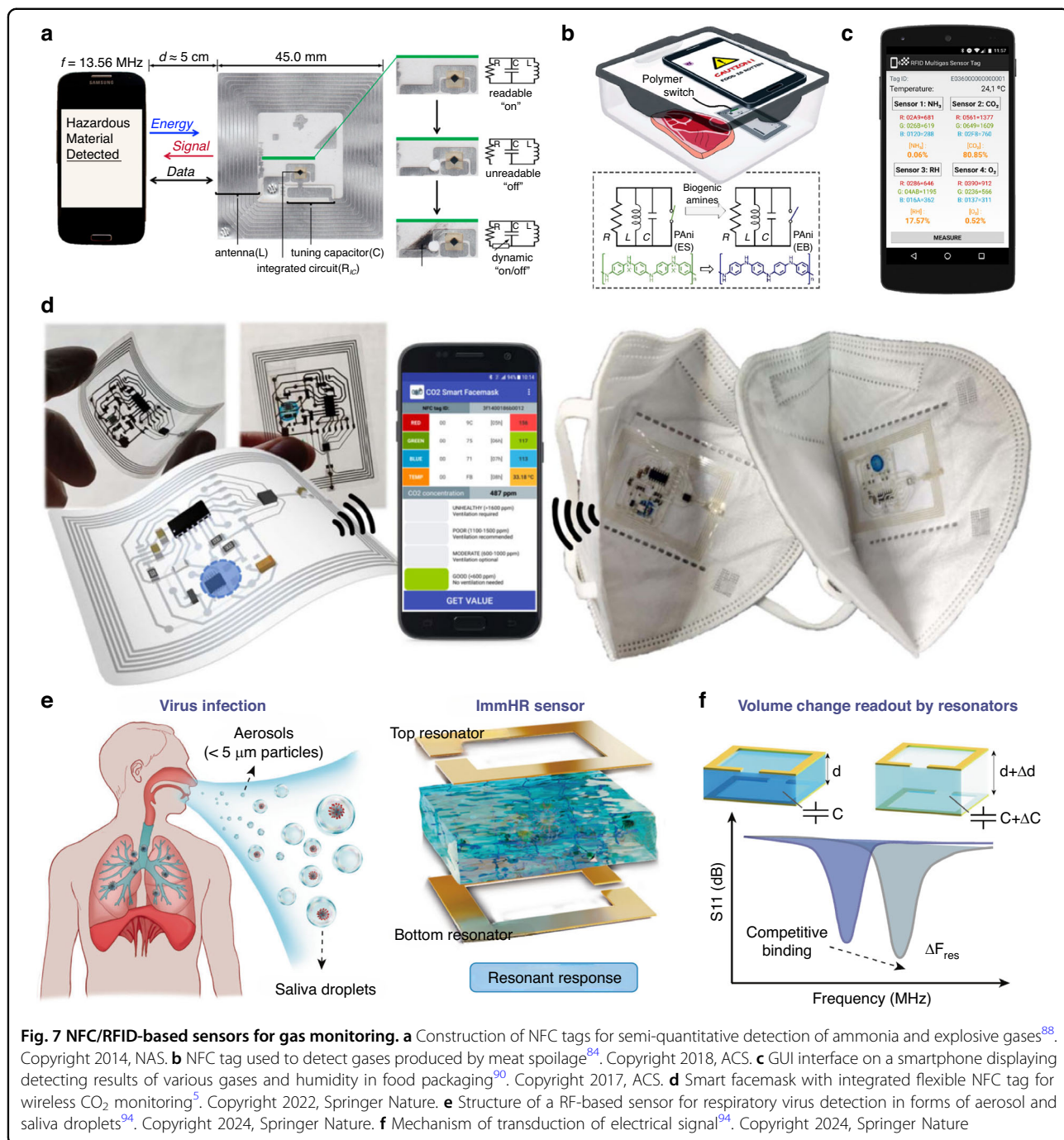


Fig. 7 NFC/RFID-based sensors for gas monitoring. **a** Construction of NFC tags for semi-quantitative detection of ammonia and explosive gases⁸⁸. Copyright 2014, NAS. **b** NFC tag used to detect gases produced by meat spoilage⁸⁴. Copyright 2018, ACS. **c** GUI interface on a smartphone displaying detecting results of various gases and humidity in food packaging⁹⁰. Copyright 2017, ACS. **d** Smart facemask with integrated flexible NFC tag for wireless CO₂ monitoring⁵. Copyright 2022, Springer Nature. **e** Structure of a RF-based sensor for respiratory virus detection in forms of aerosol and saliva droplets⁹⁴. Copyright 2024, Springer Nature. **f** Mechanism of transduction of electrical signal⁹⁴. Copyright 2024, Springer Nature

particularly in terms of transduction mechanisms and integration strategies. This similarity enables the adaptation of NFC-based gas sensor platforms for real-time, non-invasive monitoring of aerosol-borne biomarkers, such as respiratory viruses. Figure 7e shows a wireless RF-based immunoassay system uses an immuno-responsive hydrogel-modulated resonant (ImmHR) sensor for rapid virus detection (e.g., SARS-CoV-2, H1N1, RSV)⁹⁴. The hydrogel, grafted with viral antigens and antibody-

conjugated gold nanoparticles, swells upon antigen binding, altering the dielectric constant between paired RF resonators (Fig. 7f). This shifts the resonant frequency, enabling high sensitivity (limit of detection down to fg/L) and fast detection (<10 min) while minimizing environmental interference. Such integration of NFC-based sensors into smart devices opens new possibilities for real-time, non-invasive health monitoring and pathogen detection.

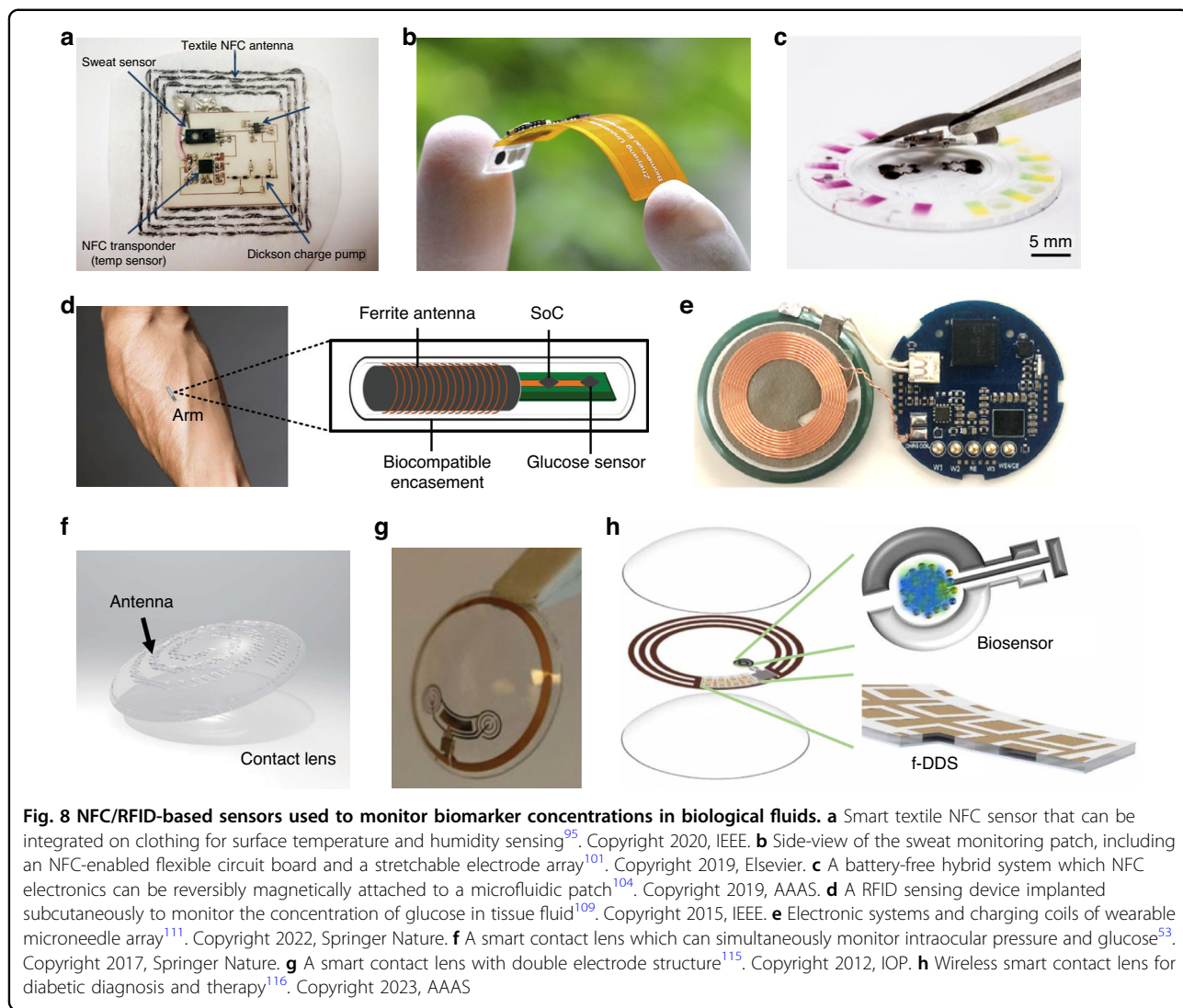


Fig. 8 NFC/RFID-based sensors used to monitor biomarker concentrations in biological fluids. **a** Smart textile NFC sensor that can be integrated on clothing for surface temperature and humidity sensing⁹⁵. Copyright 2020, IEEE. **b** Side-view of the sweat monitoring patch, including an NFC-enabled flexible circuit board and a stretchable electrode array¹⁰¹. Copyright 2019, Elsevier. **c** A battery-free hybrid system which NFC electronics can be reversibly magnetically attached to a microfluidic patch¹⁰⁴. Copyright 2019, AAAS. **d** A RFID sensing device implanted subcutaneously to monitor the concentration of glucose in tissue fluid¹⁰⁹. Copyright 2015, IEEE. **e** Electronic systems and charging coils of wearable microneedle array¹¹¹. Copyright 2022, Springer Nature. **f** A smart contact lens which can simultaneously monitor intraocular pressure and glucose⁵³. Copyright 2017, Springer Nature. **g** A smart contact lens with double electrode structure¹¹⁵. Copyright 2012, IOP. **h** Wireless smart contact lens for diabetic diagnosis and therapy¹¹⁶. Copyright 2023, AAAS

Sensors for metabolites monitoring in biofluid

Biological fluids, such as sweat, urine, tears, and blood, are rich in biomarkers like metabolites, electrolytes, proteins, and heavy metals making them invaluable for rapid disease screening and health management. Current NFC sensors often focus on monitoring fluid volume using commercial humidity sensors (Fig. 8a)⁹⁵ or capacitive sensing methods⁹⁶. However, these sensors primarily assess the wearer's condition based on body fluid volume and lack quantitative biomarker analysis. Therefore, there is a demand for sensors that can quantitatively detect specific biomarkers in biological fluids to enhance disease detection and prevention. Recent advancements have shown promise in this area. The modified electrode arrays have been used to quantitatively detect biomarkers in sweat by means of electrochemical sensing^{16,97,98}. Despite these advances, some sweat sensors^{99,100} still rely on batteries to power the device, which limits their

miniaturization and flexibility. To address the limitation, a wireless passive electrochemical sensing patch based on NFC technology has been developed, including different electrochemically modified electrode arrays on the surface (Fig. 8b)¹⁰¹. The thin and flexible NFC antenna provides energy for the sensor patch wirelessly. Antenna and electronic components are integrated onto a flexible circuit board, improving system integration and reducing device size¹⁰¹. The electrode array can be modified with ionic sensitive films to detect the concentrations of various ions (Na^+ , K^+ , H^+ , Ca^{2+} , Cl^-) and glucose in sweat^{101–103}. Furthermore, the introduction of microfluidic channels, as demonstrated by Bandodkar et al., enables efficient sweat distribution across multiple electrodes, facilitating multimodal sensing. (Fig. 8c)¹⁰⁴. The sweat is collected and transported to individual chambers by a microfluidic substrate that houses electrochemical sensing electrodes and a variety of colorimetric assays that

simultaneously detect lactic acid, glucose, chloride, pH, and sweat rate.

Based on the strong correlation between the glucose concentrations in interstitial fluid and tears with blood glucose levels^{105–108}, many wireless glucose sensors are reported. Approaches for monitoring tissue fluid glucose can be categorized into subcutaneous implantation, reverse iontophoresis, and microneedle sampling. Subcutaneous implants allow continuous monitoring of biomarkers in tissue fluid. An RFID-based subcutaneous implant device can continuously monitor blood glucose concentration in tissue fluid (Fig. 8d)¹⁰⁹, but it remains invasive and poses risks such as infection and biocompatibility issues. In contrast, reverse iontophoresis allows non-invasive extraction of interstitial fluid using a mild current between two electrodes on the skin surface¹¹⁰. Another solution is to collect interstitial fluid through wearable microneedles. Tehrani et al. have reported a wireless wearable microneedle sensor array (microneedle diameter: ~200 μm) for monitoring multiple biomarkers (alcohol, glucose, and lactate) in interstitial fluid, and charges its battery via a near-field coil (Fig. 8e)¹¹¹.

The glucose concentration in tears is also closely related to the blood sugar level¹¹². Unlike traditional wired transmission methods, which can obstruct vision and increase infection risks, smart contact lenses with RFID coils and chemically modified electrodes provide a practical solution for wireless tear sensing (Fig. 8f)⁵³. The highly sensitive detection of glucose is generally achieved through glucose oxidase modified electrode^{113,114}. To further enhance the selectivity, there are contact lenses can compensate for interfering electroactive substances in tears by using a dual-sensor structure (one activates glucose oxidase, and the other deactivates it)¹¹⁵, thereby improving the sensor's accuracy (Fig. 8g). Additionally, smart contact lenses can also integrate chips and flexible drug delivery systems that can be wirelessly controlled (Fig. 8h), enabling real-time biosensing of ocular biomarkers and on-demand drug treatment for eye treatments¹¹⁶.

NFC/RFID-based drug delivery systems

Integrating NFC/RFID antennas into drug delivery systems (DDS) is an emerging direction in personalized medicine, enabling real-time drug delivery, diagnosis-therapy closed-loop systems, enhanced flexibility and miniaturization for wearables and implants. Radio frequency waves from external coils serve two main functions in DDS: enabling communication and powering the DDS^{117,118}, and directly stimulating the DDS for drug release²⁸. The former application is typically employed in wearable NFC drug delivery patches, while the latter is more commonly applied in implantable RFID drug delivery devices.

In wound healing applications, NFC technology enables the creation of smart wound dressings that can monitor wounds and deliver drugs without adding bulk. For instance, a wireless passive NFC-based smart wound dressing has been developed to track temperature, pH, and uric acid levels on the wound surface¹¹⁹ (Fig. 9a). This represents a significant advancement over earlier smart dressings that monitored only a single parameter, such as temperature¹²⁰ or pH¹²¹, allowing for a more accurate assessment of the infection status. Data collected from the dressing is transmitted to a smartphone, which evaluates drug delivery needs, and the smart dressing releases the drug via an electric signal-controlled module. Another example is a wireless closed-loop smart dressing that releases drugs based on feedback from wound temperature and humidity, using heated liquid metal coils to trigger the release of drugs encapsulated in thermosensitive hydrogels (Fig. 9b)¹². Beyond wound care, wearable NFC patches have been used in the treatment of neurological diseases by electrically triggering drug release via microneedles¹²².

Epidermal NFC drug delivery patches are primarily used for monitoring and treating surface wounds due to the skin barrier, which often results in slow drug release rates and limited drug options¹²³. However, many diseases necessitate targeted intracorporeal drug delivery, where implantable NFC/RFID-based systems can offer rapid and precise therapy^{124–127}. For instance, implantable devices with flexible radio frequency antennas can harvest energy through inductive coupling from an external coil, which can be used to heat and drive drug release for treatments like brain tumor therapy¹²⁶. Another strategy is to convert the radio frequency signals received by the RFID antenna into direct current voltage, which can chemically degrade the metal layer encapsulating the drug^{128,129} or generate gas through water electrolysis to trigger the drug release (Fig. 9c)¹¹. Noted that, the use of coils with different resonant frequencies is controllable which can allow for multiple, sequential drug releases (Fig. 9d, e)¹²⁹.

Biocompatibility is crucial for implantable radio frequency drug delivery devices. Researchers have proposed a biodegradable wireless power supply system with excellent biocompatibility, delivering direct current voltage for in-body wireless drug delivery. Apart from the rectifier module, the coils, wires, and capacitors are made from biodegradable materials. When placed in a phosphate-buffered saline (PBS) solution (pH 7.4, 80 °C), the Mg interconnect wire and receiver coil fully dissolved after 15 days, followed by the degradation of the Zn negative electrode and MoS₂/rGO positive electrode of the capacitor into negligible black spots over the next 40 days (Fig. 9f)¹³⁰. This illustrates the potential of biodegradable materials for implantable bioelectronic applications.

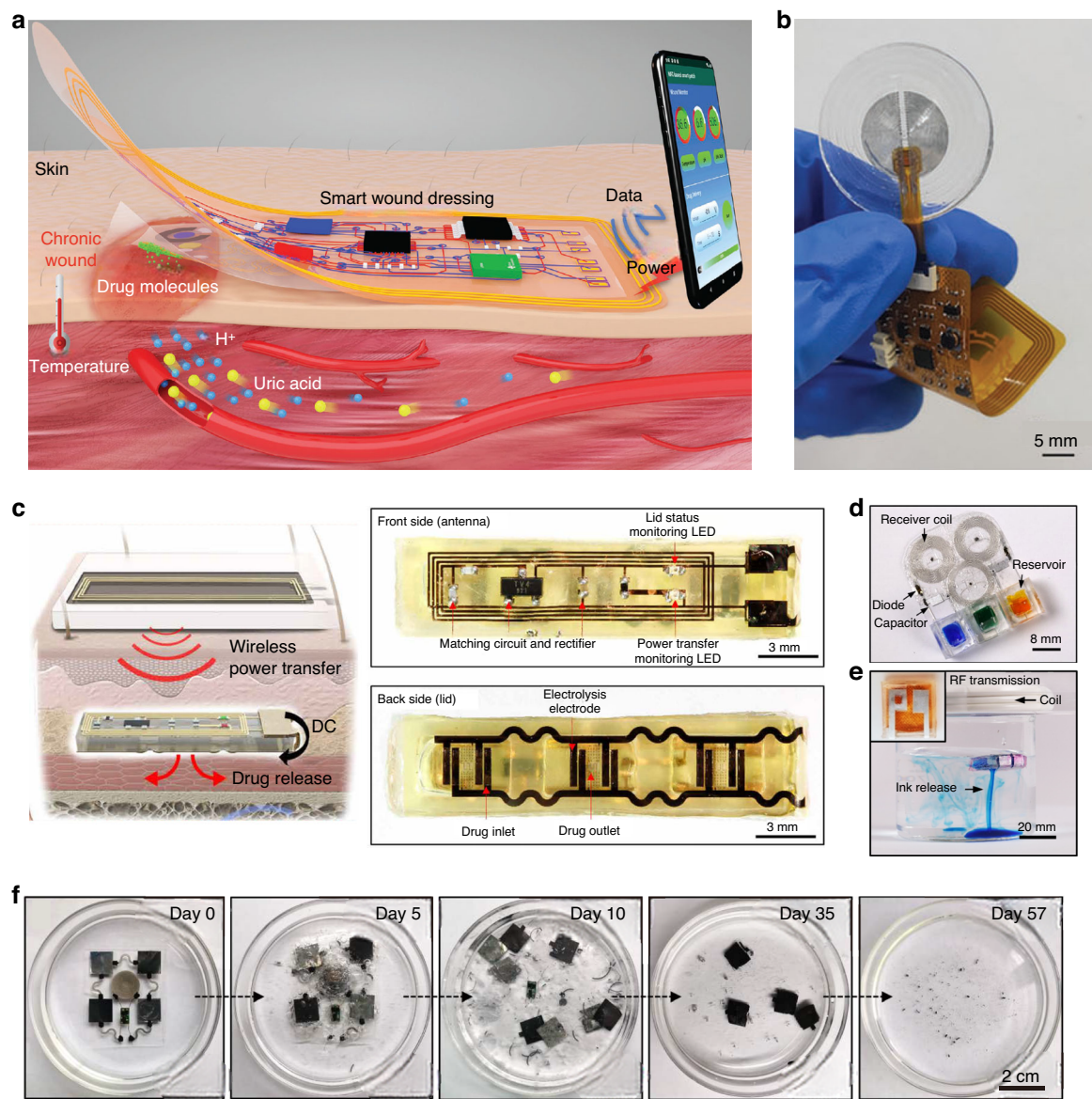
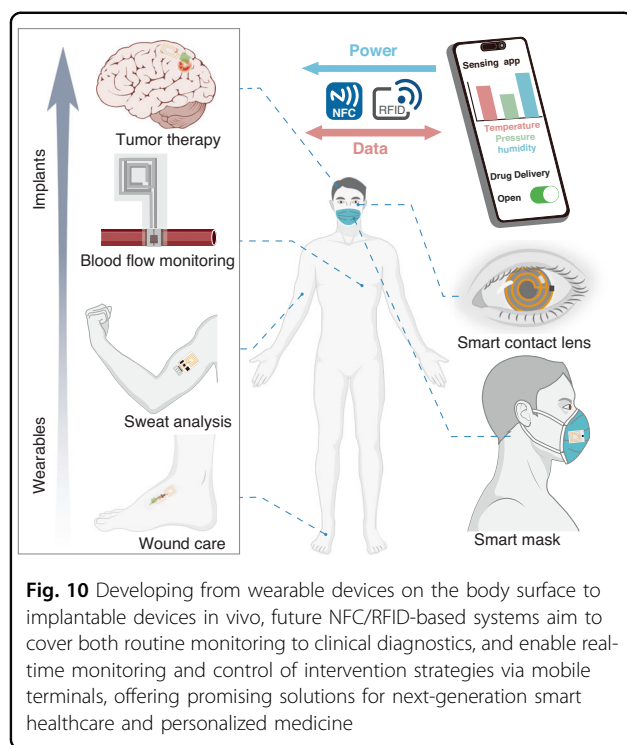


Fig. 9 NFC/RFID-based wearable and implantable drug delivery systems. **a** A smart wound dressing that detects the various physiological parameters of the wound surface and delivers drugs¹¹⁹. Copyright 2021, Wiley-VCH. **b** A wireless and closed-loop smart dressing that releases drugs by heating liquid metal coils¹². Copyright 2023, Wiley-VCH. **c** Schematic illustration of a soft, wireless implantable drug delivery system in the subcutaneous region with images of the front and backside of the system¹¹. Copyright 2021, AAAS. **d** The biodegradable RF drug delivery device can realize multiple drug delivery¹²⁹. Copyright 2020, AAAS. **e** Drug release simulation¹²⁹. Copyright 2020, AAAS. **f** The degradation process of a soft implantable energy supply system that can be charged wirelessly¹³⁰. Copyright 2023, AAAS

Conclusion and perspective

The integration of NFC/RFID technology into flexible sensing systems has overcome the limitations of wired connections and bulky power supplies, driving the development of personalized, multifunctional wearables and implants. NFC/RFID-based sensors facilitate real-time, noninvasive monitoring of diverse health related physiological indicators, enable real-time, noninvasive monitoring of various physiological indicators,

including intraocular pressure, strain, electrophysiological, and biochemical parameters, enhancing personalized health management with their convenience and versatility. Implantable applications further broaden their utility by capturing physiological signals within the human body. Integrating drug delivery function with sensors further empower closed-loop diagnosis and therapy capabilities to the NFC/RFID-based wearables and implants.



Despite significant progress in developing NFC/RFID-based functional systems, several challenges remain. For antenna systems, data or power transmission efficiency is highly dependent on factors such as antenna shape, conductivity, alignment, and distance changes. In flexible sensors, ensuring mechanical compliance presents significant challenges to maintain system stability. Driven by the pursuit of higher integration and miniaturization, NFC/RFID-based bio/chemical sensors are facing increasing challenges, including accurate detection of multiple biomarkers, transition from qualitative to high-precision quantitative sensing, and management of the complexity associated with monitoring diverse physiological parameters. In implants applications, extra challenges brought by the implantable devices *in vivo*, such as the signal attenuation and distortion within the body still need to be addressed (Fig. 10). Moreover, power transmission and data exchange can generate heat, which is a concern for implantable sensors as it can damage surrounding tissues or cause discomfort.

Beyond technical barriers, the commercialization of NFC/RFID-based biomedical devices must also contend with multifaceted challenges related to safety and regulatory compliance. Electromagnetic compatibility is a critical concern, as NFC/RFID signals may interfere with sensitive medical equipment like pacemakers and infusion pumps, necessitating rigorous EMI testing and conformance to compatibility standards. The wireless nature

of these systems also introduces data privacy and cybersecurity risks; without strong encryption and authentication, patient information may be vulnerable to unauthorized access. Regulatory frameworks for such devices vary globally—for instance, the U.S. FDA classifies certain RFID-enabled medical devices as Class II, subject to strict safety and performance evaluations. Similar requirements exist in the EU, China, and other regions, with differences in frequency bands, power constraints, and certification processes. Therefore, successful clinical translation requires not only technological innovation, but also proactive regulatory navigation and robust implementation of safety and data protection strategies.

These challenges together form a roadmap for future research (Fig. 10). The development of new functional materials (highly stretchable, conductive, while ideally, be bioabsorbable) and innovations in antenna design will not only address current limitations but also set the stage for future advancements. In addition, commercialization and clinical application of these sensors involves further reducing manufacturing costs through the maturation of flexible electronics manufacturing technologies, thus facilitating the transition from concept to practical wearable devices. As flexible sensors become more integrated with mobile health applications, cloud computing, and artificial intelligence, they will be able to offer more personalized health management solutions. We believe that as technology continues to evolve and market demand increases, flexible NFC/RFID-based wearable and implantable systems will make significant contributions to medical care by improving health management and patient outcomes.

Acknowledgements

The authors thank the financial support from the National Natural Science Foundation of China (62235008), Natural Science Foundation for Excellent Young Scholars (62322108), National Key R&D Program of China under Grant (2021YFB3601200), Natural Science Foundation for Young Scholars (62201286, 62301283, 22405131), the Program of Jiangsu Specially-Appointed Professor, Jiangsu Funding Program for Excellent Postdoctoral Talent (2023ZB587), Nanjing U35 Program, Natural Science Research Start-up Foundation of Recruiting Talents of Nanjing University of Posts and Telecommunications (NY222099). Haochen Zou, Zhibo Zhou and Mengyao Huang contributed equally to this work.

Conflict of interest

The authors declare no competing interests.

Received: 31 March 2025 Revised: 21 May 2025 Accepted: 15 June 2025

Published online: 23 October 2025

References

- Zhang, P., Zhu, B., Du, P. & Travas-Sejdic, J. Electrochemical and electrical biosensors for wearable and implantable electronics based on conducting polymers and carbon-based materials. *Chem. Rev.* **124**, 722–767 (2024).
- Kim, J. et al. A soft and transparent contact lens for the wireless quantitative monitoring of intraocular pressure. *Nat. Biomed. Eng.* **5**, 772–782 (2021).

3. Kwon, K. et al. A battery-less wireless implant for the continuous monitoring of vascular pressure, flow rate and temperature. *Nat. Biomed. Eng.* **7**, 1215–1228 (2023).
4. Lin, R. et al. Digitally-embroidered liquid metal electronic textiles for wearable wireless systems. *Nat. Commun.* **13**, 2190 (2022).
5. Escobedo, P. et al. Smart facemask for wireless CO₂ monitoring. *Nat. Commun.* **13**, 72 (2022).
6. Yang, C. et al. Intelligent wireless theranostic contact lens for electrical sensing and regulation of intraocular pressure. *Nat. Commun.* **13**, 2556 (2022).
7. Galli, V. et al. Passive and wireless all-textile wearable sensor system. *Adv. Sci.* **10**, 2206665 (2023).
8. Boutry, C. M. et al. Biodegradable and flexible arterial-pulse sensor for the wireless monitoring of blood flow. *Nat. Biomed. Eng.* **3**, 47–57 (2019).
9. Kalidasan, V. et al. Wirelessly operated bioelectronic sutures for the monitoring of deep surgical wounds. *Nat. Biomed. Eng.* **5**, 1217–1227 (2021).
10. Ruth, S. R. A. et al. Post-surgical wireless monitoring of arterial health progression. *iScience* **24**, 103079 (2021).
11. Joo, H. et al. Soft implantable drug delivery device integrated wirelessly with wearable devices to treat fatal seizures. *Sci. Adv.* **7**, eabd4639 (2021).
12. Ge, Z. et al. Wireless and closed-loop smart dressing for exudate management and on-demand treatment of chronic wounds. *Adv. Mater.* **35**, 2304005 (2023).
13. Chung, H. U. et al. Binodal, wireless epidermal electronic systems with in-sensor analytics for neonatal intensive care. *Science* **363**, eaau0780 (2019).
14. Li, J. et al. Thin, soft, wearable system for continuous wireless monitoring of artery blood pressure. *Nat. Commun.* **14**, 5009 (2023).
15. Oh, Y. S. et al. Battery-free, wireless soft sensors for continuous multi-site measurements of pressure and temperature from patients at risk for pressure injuries. *Nat. Commun.* **12**, 5008 (2021).
16. Gao, W. et al. Fully integrated wearable sensor arrays for multiplexed in situ perspiration analysis. *Nature* **529**, 509–514 (2016).
17. Coskun, V., Ozdenizci, B. & Ok, K. A survey on Near Field Communication (NFC) technology. *Wirel. Pers. Commun.* **71**, 2259–2294 (2012).
18. Park, S. I. et al. Soft, stretchable, fully implantable miniaturized optoelectronic systems for wireless optogenetics. *Nat. Biotechnol.* **33**, 1280–1286 (2015).
19. Di Renzo, F., Virdis, A., Vallati, C., Carbonaro, N. & Tognetti, A. Evaluation of NFC-enabled devices for heterogeneous wearable biomedical application. *IEEE J. Radio Freq. Identif.* **4**, 373–383 (2020).
20. Kong, L. et al. Wireless technologies in flexible and wearable sensing: from materials design, system integration to applications. *Adv. Mater.* **36**, 2400333 (2024).
21. DeHennis, A., Getzlaff, S., Grice, D. & Mailand, M. An NFC-enabled CMOS IC for a wireless fully implantable glucose sensor. *IEEE J. Biomed. Health Inform.* **20**, 18–28 (2016).
22. Li, K. et al. A generic soft encapsulation strategy for stretchable electronics. *Adv. Funct. Mater.* **29**, 1806630 (2019).
23. Shao, Y. Z. et al. Room-temperature high-precision printing of flexible wireless electronics based on MXene inks. *Nat. Commun.* **13**, 3223 (2022).
24. Ji, B. et al. Recent advances in wireless epicortical and intracortical neuronal recording systems. *Sci. China Inf. Sci.* **65**, 140401 (2022).
25. Flynn, C. D. et al. Biomolecular sensors for advanced physiological monitoring. *Nat. Rev. Bioeng.* **1**, 560–575 (2023).
26. Kim, J., Campbell, A. S., de Ávila, B. E.-F. & Wang, J. Wearable biosensors for healthcare monitoring. *Nat. Biotechnol.* **37**, 389–406 (2019).
27. Kim, J. et al. Skin-interfaced wireless biosensors for perinatal and paediatric health. *Nat. Rev. Bioeng.* **1**, 631–647 (2023).
28. Mirvakili, S. M. & Langer, R. Wireless on-demand drug delivery. *Nat. Electron.* **4**, 464–477 (2021).
29. Sunwoo, S.-H. et al. Soft bioelectronics for the management of cardiovascular diseases. *Nat. Rev. Bioeng.* **2**, 8–24 (2024).
30. Olenik, S., Lee, H. S. & Güder, F. The future of near-field communication-based wireless sensing. *Nat. Rev. Mater.* **6**, 286–288 (2021).
31. Biswas, K., Sinclair, M., Hyde, J. & Mahbub, I. An NFC (near-field communication) based wireless power transfer system design with miniaturized receiver coil for optogenetic implants. In *Proc. 2018 Texas Symp. Wireless and Microwave Circuits and Systems (WMCS)*. IEEE, 1–5 (2018).
32. Jawad, A. M., Nordin, R., Gharghan, S. K., Jawad, H. M. & Ismail, M. Opportunities and challenges for near-field wireless power transfer: A review. *Energies* **10**, 1022 (2017).
33. Kim, H. J. et al. Review of near-field wireless power and communication for biomedical applications. *IEEE Access* **5**, 21264–21285 (2017).
34. Gu, W., Luong, K., Yao, Z., Cui, H. & Wang, Y. E. Ferromagnetic resonance-enhanced electrically small antennas. *IEEE Trans. Antennas Propag.* **69**, 8304–8314 (2021).
35. Hong, S. et al. Dual-directional near field communication tag antenna with effective magnetic field isolation from wireless power transfer system. In *Proc. 2017 IEEE Wireless Power Transfer Conference (WPTC)*. IEEE, 1–3 (2017).
36. Saggin, B. et al. Validation of a simple metabolic-equivalent-of-task sensor based on a low-cost NFC RFID wristband. *IEEE Sens. J.* **19**, 353–360 (2019).
37. Escobedo, P., Bhattacharjee, M., Nikbakhtnasrabadi, F. & Dahiya, R. Smart bandage with wireless strain and temperature sensors and batteryless NFC tag. *IEEE Internet Things J.* **8**, 5093–5100 (2021).
38. Niu, S. et al. A wireless body area sensor network based on stretchable passive tags. *Nat. Electron.* **2**, 361–368 (2019).
39. Williams, D. F. On the mechanisms of biocompatibility. *Biomaterials* **29**, 2941–2953 (2008).
40. La Mattina, A. A., Mariani, S. & Barillaro, G. Bioresorbable materials on the rise: from electronic components and physical sensors to in vivo monitoring systems. *Adv. Sci.* **7**, 1902872 (2020).
41. Balanis, C. A. *Antenna Theory: Analysis and Design* (John Wiley, 2016).
42. Rajendran, D. & Kanour, O. A comparative study of simulation methods for patch antenna strain sensors. In *Proc. 2022 19th International Multi-Conference on Systems, Signals & Devices (SSD)*. IEEE, 207–211 (2022).
43. Mevada, P., Sharma, A. K., Kulshrestha, S., Chakrabarty, S. & Jyoti, R. Frequency agile monolithic inset fed microstrip patch antenna based on barium strontium titanate ($\text{Ba}_x\text{Sr}_{1-x}\text{TiO}_3$) ferroelectric substrate. In: *2017 IEEE MTT-S International Microwave and RF Conference (IMaRC)*. IEEE, 1–5 (2017).
44. Sridhar, V. & Takahata, K. A hydrogel-based passive wireless sensor using a flex-circuit inductive transducer. *Sens. Actuators, A* **155**, 58–65 (2009).
45. Ren, Q. Y., Wang, L. F., Huang, J. Q., Zhang, C. & Huang, Q. A. Simultaneous remote sensing of temperature and humidity by LC-type passive wireless sensors. *J. Microelectromech. Syst.* **24**, 1117–1123 (2015).
46. Cañó, J. I., Bonache, J., Paredes, F. & Martín, F. Reconfigurable system for Wireless Power Transfer (WPT) and Near Field Communications (NFC). *IEEE J. Radio Freq. Identif.* **1**, 253–259 (2017).
47. Jow, U. M. & Ghovalloo, M. Design and optimization of printed spiral coils for efficient transcutaneous inductive power transmission. *IEEE Trans. Biomed. Circuits Syst.* **1**, 193–202 (2007).
48. Pascolini, D. & Mariotti, S. P. Global estimates of visual impairment: 2010. *Br. J. Ophthalmol.* **96**, 614–618 (2012).
49. Duan, Z. et al. An ultrasensitive Ti₃C₂T MXene-based soft contact lens for continuous and nondestructive intraocular pressure monitoring. *Small* **20**, 2309785 (2024).
50. Ren, X. et al. Contact lens sensor with anti-jamming capability and high sensitivity for intraocular pressure monitoring. *ACS Sens.* **8**, 2691–2701 (2023).
51. Kim, J. et al. Intraocular pressure monitoring following islet transplantation to the anterior chamber of the eye. *Nano Lett.* **20**, 1517–1525 (2020).
52. Zhu, H. et al. Hydrogel-based smart contact lens for highly sensitive wireless intraocular pressure monitoring. *ACS Sens.* **7**, 3014–3022 (2022).
53. Kim, J. et al. Wearable smart sensor systems integrated on soft contact lenses for wireless ocular diagnostics. *Nat. Commun.* **8**, 14997 (2017).
54. Kim, T. Y. et al. Wireless theranostic smart contact lens for monitoring and control of intraocular pressure in glaucoma. *Nat. Commun.* **13**, 6801 (2022).
55. Yu, X. et al. Skin-integrated wireless haptic interfaces for virtual and augmented reality. *Nature* **575**, 473–479 (2019).
56. Chen, S., Song, Y., Ding, D., Ling, Z. & Xu, F. Flexible and anisotropic strain sensor based on carbonized crepe paper with aligned cellulose fibers. *Adv. Funct. Mater.* **28**, 1802547 (2018).
57. Sun, R. et al. Magnetically induced robust anisotropic structure of multi-walled carbon nanotubes/Ni for high-performance flexible strain sensor. *Carbon* **194**, 185–196 (2022).
58. Ma, C. et al. Ultrasensitive, highly selective, integrated multidimensional sensor based on a rigid-flexible synergistic stretchable substrate. *Adv. Fiber Mater.* **5**, 1392–1403 (2023).
59. Yang, H. et al. Wireless Ti_{(3)C₂T_(x)} MXene strain sensor with ultrahigh sensitivity and designated working windows for soft exoskeletons. *ACS Nano* **14**, 11860–11875 (2020).
60. Xu, L. et al. Moisture-resilient graphene-dyed wool fabric for strain sensing. *ACS Appl. Mater. Interfaces* **12**, 13265–13274 (2020).

61. Hajighajani, A. et al. Textile-integrated metamaterials for near-field multi-body area networks. *Nat. Electron.* **4**, 808–817 (2021).
62. Lin, R. et al. Wireless battery-free body sensor networks using near-field-enabled clothing. *Nat. Commun.* **11**, 444 (2020).
63. Matsuhisa, N. et al. High-frequency and intrinsically stretchable polymer diodes. *Nature* **600**, 246–252 (2021).
64. Kim, S. H. et al. Strain-invariant stretchable radio-frequency electronics. *Nature* **629**, 1047–1054 (2024).
65. Dargaville, T. R. et al. Sensors and imaging for wound healing: a review. *Biosens. Bioelectron.* **41**, 30–42 (2013).
66. Zhang, J., Li, Y. & Xing, Y. Ultrasoft, adhesive and millimeter scale epidermis electronic sensor for real-time enduringly monitoring skin strain. *Sensors* **19**, 2442 (2019).
67. Cho, S. et al. Wireless, multimodal sensors for continuous measurement of pressure, temperature, and hydration of patients in wheelchair. *npj Flex. Electron.* **7**, 8 (2023).
68. Han, H. et al. Battery-free, wireless, ionic liquid sensor arrays to monitor pressure and temperature of patients in bed and wheelchair. *Small* **19**, 2205048 (2023).
69. Choi, J. et al. Customizable, conformal, and stretchable 3D electronics via predistorted pattern generation and thermoforming. *Sci. Adv.* **7**, eabj0694 (2021).
70. Han, S. et al. Battery-free, wireless sensors for full-body pressure and temperature mapping. *Sci. Transl. Med.* **10**, eaan4950 (2018).
71. Kwak, J. W. et al. Wireless sensors for continuous, multimodal measurements at the skin interface with lower limb prostheses. *Sci. Transl. Med.* **12**, eabc4327 (2020).
72. Li, J. et al. An ultrasensitive multimodal intracranial pressure biotelemetric system enabled by exceptional point and iontronics. *Nat. Commun.* **15**, 9557 (2024).
73. Zhang, H. et al. Wireless, battery-free optoelectronic systems as subdermal implants for local tissue oximetry. *Sci. Adv.* **5**, eaaw0873 (2019).
74. Cai, X. et al. A wireless optoelectronic probe to monitor oxygenation in deep brain tissue. *Nat. Photonics* **18**, 492–500 (2024).
75. Rigo, B. et al. Soft implantable printed bioelectronic system for wireless continuous monitoring of restenosis. *Biosens. Bioelectron.* **241**, 115650 (2023).
76. Herbert, R., Lim, H.-R., Rigo, B. & Yeo, W.-H. Fully implantable wireless batteryless vascular electronics with printed soft sensors for multiplex sensing of hemodynamics. *Sci. Adv.* **8**, eabm1175 (2022).
77. Wang, S. et al. A self-assembled implantable microtubular pacemaker for wireless cardiac electrophysiology. *Sci. Adv.* **9**, eadj0540 (2023).
78. Kang, S. K. et al. Bioreversible silicon electronic sensors for the brain. *Nature* **530**, 71–76 (2016).
79. Ausra, J. et al. Wireless, fully implantable cardiac stimulation and recording with on-device computation for closed-loop pacing and defibrillation. *Sci. Adv.* **8**, eabq7469 (2022).
80. Ouyang, W. et al. A wireless and battery-less implant for multimodal closed-loop neuromodulation in small animals. *Nat. Biomed. Eng.* **7**, 1252–1269 (2023).
81. Van Toan, N. et al. Enhanced NH₃ and H₂ gas sensing with H₂S gas interference using multilayer SnO₂/Pt/WO₃ nanofilms. *J. Hazard. Mater.* **412**, 125181 (2021).
82. Chen, Y. et al. Hierarchical flower-like TiO₂ microspheres for high-selective NH₃ detection: a density functional theory study. *Sens. Actuators, B* **345**, 130303 (2021).
83. Zhu, R., Desroches, M., Yoon, B. & Swager, T. M. Wireless oxygen sensors enabled by Fe(ii)-polymer wrapped carbon nanotubes. *ACS Sens.* **2**, 1044–1050 (2017).
84. Ma, Z. et al. Highly sensitive, printable nanostructured conductive polymer wireless sensor for food spoilage detection. *Nano Lett.* **18**, 4570–4575 (2018).
85. Chen, H. et al. Wearable dual-signal NH₃ sensor with high sensitivity for non-invasive diagnosis of chronic kidney disease. *Langmuir* **39**, 3420–3430 (2023).
86. Li, Y. et al. Wearable gas sensor based on reticular antimony-doped SnO₂/PANI nanocomposite realizing intelligent detection of ammonia within a wide range of humidity. *ACS Sens.* **8**, 4132–4142 (2023).
87. Wang, Z. et al. 2D PtSe₂ enabled wireless wearable gas monitoring circuits with distinctive strain-enhanced performance. *ACS Nano* **17**, 11557–11566 (2023).
88. Azzarelli, J. M., Mirica, K. A., Ravnsbaek, J. B. & Swager, T. M. Wireless gas detection with a smartphone via rf communication. *Proc. Natl. Acad. Sci. USA* **111**, 18162–18166 (2014).
89. Xu, G. et al. Passive and wireless near field communication tag sensors for biochemical sensing with smartphone. *Sens. Actuators, B* **246**, 748–755 (2017).
90. Escobedo, P. et al. Flexible passive near field communication tag for multigas sensing. *Anal. Chem.* **89**, 1697–1703 (2017).
91. Das, S. & Pal, M. Review-non-invasive monitoring of human health by exhaled breath analysis: a comprehensive review. *J. Electrochem. Soc.* **167**, 037562 (2020).
92. Le Maout, P. et al. Polyaniline nanocomposites based sensor array for breath ammonia analysis. Portable e-nose approach to non-invasive diagnosis of chronic kidney disease. *Sens. Actuators B* **274**, 616–626 (2018).
93. Zhao, H. et al. Proton-conductive gas sensor: A new way to realize highly selective ammonia detection for analysis of exhaled human breath. *ACS Sens.* **5**, 346–352 (2020).
94. Li, X. et al. Rapid and on-site wireless immunoassay of respiratory virus aerosols via hydrogel-modulated resonators. *Nat. Commun.* **15**, 4035 (2024).
95. Jiang, Y., Pan, K., Leng, T. & Hu, Z. Smart textile integrated wireless powered near field communication body temperature and sweat sensing system. *IEEE J. Electromagn. RF Microw. Med. Biol.* **4**, 164–170 (2020).
96. Lazar, A., Boada, M., Villarino, R. & Girbau, D. Battery-less smart diaper based on NFC technology. *IEEE Sens. J.* **19**, 10848–10858 (2019).
97. Tu, J. et al. A wireless patch for the monitoring of C-reactive protein in sweat. *Nat. Biomed. Eng.* **7**, 1293–1306 (2023).
98. Nyein, H. Y. Y. et al. A wearable electrochemical platform for noninvasive simultaneous monitoring of Ca²⁺ and pH. *ACS Nano* **10**, 7216–7224 (2016).
99. Liu, Y. et al. Skin-interfaced superhydrophobic insensible sweat sensors for evaluating body thermoregulation and skin barrier functions. *ACS Nano* **17**, 5588–5599 (2023).
100. Honda, S., Tanaka, R., Matsumura, G., Seimiya, N. & Takei, K. Wireless, flexible, ionic, perspiration-rate sensor system with long-time and high sweat volume functions toward early-stage, real-time detection of dehydration. *Adv. Funct. Mater.* **33**, 2306156 (2023).
101. Xu, G. et al. Smartphone-based battery-free and flexible electrochemical patch for calcium and chloride ions detections in biofluids. *Sens. Actuators, B* **297** (2019).
102. Xu, G. et al. Battery-free and wireless epidermal electrochemical system with all-printed stretchable electrode array for multiplexed in situ sweat analysis. *Adv. Mater. Technol.* **4**, 2019.
103. Ma, X. et al. A monolithically integrated in-textile wristband for wireless epidermal biosensing. *Sci. Adv.* **9**, eadj2763 (2023).
104. Bandodkar, A. J. et al. Battery-free, skin-interfaced microfluidic/electronic systems for simultaneous electrochemical, colorimetric, and volumetric analysis of sweat. *Sci. Adv.* **5**, eaav3294 (2019).
105. Fogh-Andersen, N., Altura, B. M., Altura, B. T. & Siggaard-Andersen, O. J. C. C. Composition of Interstitial Fluid. *Clin. Chem.* **41**, 1522–1525 (1995).
106. Baca, J. T., Finegold, D. N. & Asher, S. A. Tear glucose analysis for the non-invasive detection and monitoring of diabetes mellitus. *Ocul. Surf.* **5**, 280–293 (2007).
107. Sen, D. K. & Sarin, G. S. Tear glucose levels in normal people and in diabetic patients. *Br. J. Ophthalmol.* **64**, 693 (1980).
108. Wu, Z. et al. Interstitial fluid-based wearable biosensors for minimally invasive healthcare and biomedical applications. *Commun. Mater.* **5**, 33 (2024).
109. Xiao, Z. et al. An implantable RFID sensor tag toward continuous glucose monitoring. *IEEE J. Biomed. Health Inform.* **19**, 910–919 (2015).
110. Baria, M., Nyein, H. Y. Y. & Javey, A. Wearable sweat sensors. *Nat. Electron.* **1**, 160–171 (2018).
111. Tehrani, F. et al. An integrated wearable microneedle array for the continuous monitoring of multiple biomarkers in interstitial fluid. *Nat. Biomed. Eng.* **6**, 1214–1224 (2022).
112. Kim, S., Jeon, H.-J., Park, S., Lee, D. Y. & Chung, E. Tear glucose measurement by reflectance spectrum of a nanoparticle embedded contact lens. *Sci. Rep.* **10**, 8254 (2020).
113. Yang, X., Pan, X., Blyth, J. & Lowe, C. R. Towards the real-time monitoring of glucose in tear fluid: holographic glucose sensors with reduced interference from lactate and pH. *Biosens. Bioelectron.* **23**, 899–905 (2008).
114. Yao, H., Shum, A. J., Cowan, M., Lähdesmäki, I. & Parviz, B. A. A contact lens with embedded sensor for monitoring tear glucose level. *Biosens. Bioelectron.* **26**, 3290–3296 (2011).
115. Yao, H. et al. A contact lens with integrated telecommunication circuit and sensors for wireless and continuous tear glucose monitoring. *J. Micromech. Microeng.* **22**, 075007 (2012).

116. Keum, D. H. et al. Wireless smart contact lens for diabetic diagnosis and therapy. *Sci. Adv.* **6**, eaba3252 (2023).
117. Wang, Q. et al. Stretchable wireless optoelectronic synergistic patches for effective wound healing. *npj Flex. Electron.* **8**, 64 (2024).
118. Nan, K. et al. An ingestible, battery-free, tissue-adhering robotic interface for non-invasive and chronic electrostimulation of the gut. *Nat. Commun.* **15**, 6749 (2024).
119. Xu, G. et al. Battery-free and wireless smart wound dressing for wound infection monitoring and electrically controlled on-demand drug delivery. *Adv. Funct. Mater.* **31** (2021).
120. Pang, Q. et al. Smart flexible electronics-integrated wound dressing for real-time monitoring and on-demand treatment of infected wounds. *Adv. Sci.* **7**, 1902673 (2020).
121. Mostafalu, P. et al. Smart bandage for monitoring and treatment of chronic wounds. *Small* **14**, e1703509 (2018).
122. Wang, Y. et al. Digital automation of transdermal drug delivery with high spatiotemporal resolution. *Nat. Commun.* **15**, 511 (2024).
123. Ye, Y., Yu, J., Wen, D., Kahkoska, A. R. & Gu, Z. Polymeric microneedles for transdermal protein delivery. *Adv. Drug Deliv. Rev.* **127**, 106–118 (2018).
124. Yin, D. et al. A battery-free nanofluidic intracellular delivery patch for internal organs. *Nature* **642**, 1051–1061 (2025).
125. Qazi, R. et al. Wireless optofluidic brain probes for chronic neuropharmacology and photostimulation. *Nat. Biomed. Eng.* **3**, 655–669 (2019).
126. Lee, J. et al. Flexible, sticky, and biodegradable wireless device for drug delivery to brain tumors. *Nat. Commun.* **10**, 5205 (2019).
127. Nie, R. et al. Implantable biophotonic device for wirelessly cancer real-time monitoring and modulable treatment. *Adv. Sci.* 2503778 <https://doi.org/10.1002/advs.202503778> (2025).
128. Sung, S. H. et al. Flexible wireless powered drug delivery system for targeted administration on cerebral cortex. *Nano Energy* **51**, 102–112 (2018).
129. Koo, J. et al. Wirelessly controlled, bioresorbable drug delivery device with active valves that exploit electrochemically triggered crevice corrosion. *Sci. Adv.* **6**, eabb1093 (2020).
130. Sheng, H. et al. A soft implantable energy supply system that integrates wireless charging and biodegradable Zn-ion hybrid supercapacitors. *Sci. Adv.* **9**, eadh8083 (2023).
131. Fiore, L. et al. Microfluidic paper-based wearable electrochemical biosensor for reliable cortisol detection in sweat. *Sens. Actuators, B* **379**, 133258 (2023).
132. Hallil, H. et al. Passive resonant sensors: trends and future prospects. *IEEE Sens. J.* **21**, 12618–12632 (2021).
133. Li, C. et al. Review of research status and development trends of wireless passive LC resonant sensors for harsh environments. *Sensors* **15**, 13097–13109 (2015).